Ark clams and relatives (Bivalvia: Arcida) show convergent morphological evolution associated with lifestyle transitions in the marine benthos

Journal:	*Biological Journal of the Linnean Society*
Manuscript ID	BJLS-5778.R1
Manuscript Type:	Original article
Date Submitted by the Author:	n/a
Complete List of Authors:	Audino, Jorge; Universidade de Sao Paulo Instituto de Biociencias, Department of Zoology Serb, JM; Iowa State University, Ecology, Evolution & Organismal Biology Marian, José; Universidade de Sao Paulo Instituto de Biociencias, Department of Zoology
Keywords:	adaptation, correlation, lifestyle, mantle, phenotype, phylogeny

Ark clams and relatives (Bivalvia: Arcida) show convergent morphological evolution associated with lifestyle transitions in the marine benthos

Jorge A. Audino[1,3], Jeanne M. Serb[2,4], and José Eduardo A. R. Marian[1,5]

[1] Department of Zoology, University of São Paulo, Rua do Matão, Travessa 14, n. 101, 05508-090 São Paulo, São Paulo, Brazil

[2] Department of Ecology, Evolution & Organismal Biology, Iowa State University, 2200 Osborn Dr., Ames, IA 50011, USA

[3] jorgeaudino@ib.usp.br (corresponding author)

[4] serb@iastate.edu

[5] jemarian@ib.usp.br

Running title: **Evolutionary convergences in ark clams and relatives (Bivalvia: Arcida)**

Abstract

One of the most intriguing questions in macroevolutionary studies is to understand how distantly related taxa can evolve towards similar phenotype in response to similar ecological conditions. Ark clams and their relatives (Arcida) display two main ecologies represented by epifaunal and infaunal lifestyles. Their mantle margin includes features, such as photosensory and muscular organs, that may coincide with each habit, making these bivalves a suitable model to explore evolutionary convergence in the marine benthos. To test for the evolutionary association between lifestyles and morphology, we gathered data on the mantle margin for 64 species across all six extant arcidan families. A molecular phylogeny of Arcida was inferred based on four gene sequences from 54 species and used to study trait evolution. Our results support that photoreceptor organs had a single origin and that infaunal lineages lost these structures in independent events, suggesting a correlated pattern of evolution. In addition, the enlargement of the posterior inner fold, which acts as a functional siphon, favored the occurrence of convergent transitions to infaunal habits during the Mesozoic. We provide evidence of ecomorphological associations and putative adaptations in a bivalve clade that sheds light into the underlying factors driving evolution of the marine benthos.

Keywords: adaptation – correlation – lifestyle – mantle – phenotype – phylogeny

Introduction

Macroevolutionary questions compose the core of evolutionary biology and focus on the association of phenotypical diversity with adaptive landscapes (Simpson, 1953; Schluter, 2000). Understanding whether and how similar ecological factors can drive independent taxa towards the same phenotype may help us better understand factors that drive evolution (Losos, 2011; Serb *et al.*, 2017). In this context, the repeated evolution of traits across independent lineages, i.e., evolutionary convergence (Agrawal, 2017), in association with similar environmental factors suggests putative adaptations and predictable responses to similar selective regimes (Harvey & Pagel, 1991; Losos, 2011; Mahler *et al.*, 2017). Whereas numerous vertebrate taxa are used as models for studies on evolutionary processes and convergence (Losos & Mahler, 2010), invertebrates are proportionally less studied, and supposed ecomorphological patterns in invertebrate taxa remain largely obscure.

Ark clams and their relatives (Bivalvia, Arcida) are marine pteriomorphian bivalves and are a suitable model to gain insights into convergent evolution due to their morphological and ecological diversity. Two main lifestyles are observed in the group (Oliver & Holmes, 2006). Epifaunal animals are attached to hard substrate (e.g., rocks and coral fragments) by a strong byssus (i.e., filaments secreted to attach the animal to solid surfaces). Alternatively, infaunal and semi-infaunal animals bury into soft sediment with the posterior region exposed above the surface. Previous anatomical studies have identified apparent associations between both modes of life with putative adaptations of shell shape, muscle organization, and photoreceptor organs (Stanley, 1972; Oliver & Holmes, 2006; Audino & Marian, 2018); however, these hypotheses were not directly tested using comparative methods.

The Arcida Gray, 1854 have a comprehensive fossil record dating back to the lower Ordovician (~450 Ma, million years ago) (Morton *et al.*, 1998; Cope, 2000). The Order currently encompasses the superfamilies Arcoidea and Limopsoidea, with an estimated diversity of more than 300 extant species (Oliver & Holmes, 2006; Carter *et al.*, 2011). The Arcoidea traditionally includes the families Arcidae, Cucullaeidae, Noetiidae, and Glycymerididae, while Limopsidae and Philobryidae are assigned to Limopsoidea (Oliver & Holmes, 2006; Carter *et al.*, 2011). Nevertheless, taxonomic classifications are controversial, with numerous morphological features likely representing homoplasies in response to similar ecologies (Oliver & Holmes, 2006).

One of these features is the mantle margin, a narrow region of soft tissues organized as lobe-like extensions lining the shell margin (Fig. 1A, B). This region is expected to evolve in response to shifts in lifestyle given that the mantle margin plays primary roles of interaction with the surrounding environment, including sensory, protective, and muscular functions (Yonge, 1983; Audino & Marian, 2016). The siphons are a classical example of a key morphological innovation in infaunal bivalves as a result of enlargement and fusion of the mantle folds. Siphons create channels for water circulation through the mantle cavity – where the gills are located – in animals that live constantly buried within the sediment (Yonge, 1983; Stanley, 1968). Other mantle structures, such as eyes and tentacles, have also been linked to ecological transitions. For instance, in scallops, depth was suggested to be an important driving force in the evolution of mantle eye components associated with light sensitivity (Malkowsky & Götze, 2014). Light-guided behaviors, e.g., related to predator detection and posture control (Nilsson, 1994), could also be associated with transitions to the epifaunal habit, *i.e.*, when the animal lives on top of the substrate. Consequently, the mantle margin in Arcida represents a promising source of information to identify convergent traits and test correlated evolution. Phenotypic diversity in number and length of mantle folds, and presence and complexity of photoreceptor organs are among key traits of this region (Waller, 1980; Morton, 1982; Morton & Peharda, 2008; Audino & Marian, 2018). Nevertheless, the structure of the mantle margin in the ancestor of ark clams and its subsequent morphological diversification have never been inferred, rendering several interesting questions. For example, did photoreceptor organs of the mantle margin evolve as adaptive traits in epifaunal groups? Are changes in mantle morphology related to shifts to the infaunal lifestyle? For instance, the enlarged posterior mantle fold of infaunal lineages may act as a functional siphon (*e.g.*, Morton, 1982) – did this attribute evolve convergently as an adaptation (or exaptation, Gould & Vrba, 1982) to the infaunal lifestyle?

A phylogenetic framework is crucial to provide initial steps towards these answers and elucidate the number of ecological transitions in the clade. Although the Arcida has been recovered monophyletic in many analyses (Steiner & Hammer, 2000; Giribet & Wheeler, 2002; Matsumoto, 2003; Bieler *et al.*, 2014), relationships among families and superfamilies remain under debate (Oliver & Holmes, 2006; Bieler *et al.*, 2014; Feng *et al.*, 2015; Combosch & Giribet, 2016). The placement of some groups, such as the Glycymerididae and the Limopsoidea, are particularly challenging (Combosch & Giribet, 2016). Consequently, a more robust phylogeny is needed to enable further evolutionary studies on the radiation of the group.

The present study provides a the most comprehensive phylogenetic analysis of Arcida to investigate morphological evolution in the clade and cast light on presumed adaptive features. Particularly, mantle margin morphology and lifestyles were studied in 64 species under a phylogenetic framework to test for correlation between lifestyle and morphology. The inferred molecular phylogenies, combined to the extensive morphological survey, provided a robust basis to discuss evolutionary patterns in the clade.

Material and Methods

Taxa sampling

Nucleotide sequences for four genes (18S rRNA, 28S rRNA, COI mtDNA, and histone H3) were obtained on GenBank for 54 species of Arcida, covering both superfamilies, all six families, and 20 genera (Table 1). The outgroup comprises seven species from other pteriomorphian orders and five species from the remaining major bivalve clades (Protobranchia and Heteroconchia) (Table 1). Missing data corresponded to 12% of the dataset for nucleotide sequences (Table 1). When possible, sampling effort was proportional to the diversity of each family, *i.e.*, relatively more samples were analyzed in groups comparatively more diverse (Table 1).

Morphological investigation of the mantle margin includes data from 64 species obtained from preserved specimens of the following collections: Museum of Comparative Zoology (MCZ), Museum of Zoology "Prof. Adão José Cardoso" of the University of Campinas (ZUECBIV), Museum of Zoology of the University of São Paulo (MZSP), Smithsonian National Museum of Natural History (USNM), and Santa Barbara Museum of Natural History (SBMNH). Respective catalog numbers are listed in Table 1. From the 64 species studied for morphology, 38 species have available sequences used for phylogenetic inference, while 26 species either belong to genera that include the remaining sequenced species or correspond to taxa included to complement the observations (Table 1). One to five specimens per species were dissected depending on the availability of preserved material.

Phylogenetic analysis and divergence times

Sequence alignments were generated with MAFFT v7.311 under the L-INS-i option (accurate strategy) (Katoh & Standley, 2013). ModelFinder (Kalyaanamoorthy *et al.*, 2017) was used to obtain the best-fit model of sequence evolution under the corrected Akaike information criterion (AICc), returning GTR + I + G for the concatenated dataset, which was applied in subsequent analyses. Maximum likelihood (ML) analysis was conducted in IQ-TREE (Nguyen *et al.*, 2014) and node support was estimated by standard nonparametric bootstrap (100 replicates) (Felsenstein, 1985). Divergence times of clades were estimated by Bayesian Inference (BI) in RevBayes v.1.0.9 under the fossilized birth-death model (Heath, Huelsenbeck,

& Stadler, 2014; Höhna *et al.*, 2016). This model imposes a time structure on the tree by marginalizing over all possible attachment points for the fossils on the extant tree. In addition, instead of treating the calibration density as an additional prior distribution on the tree, the model treats it as the likelihood of the fossil data given the tree parameter (Heath *et al.*, 2014).

Following Bieler *et al.* (2014), the root age for Bivalvia was constrained applying a uniform distribution prior between 520.5 and 530 Ma based on the fossil *Fordilla troyensis* (Pojeta *et al.*, 1973). Four additional fossils were used to calibrate internal node ages, three of them previously adopted elsewhere (Combosch & Giribet, 2016). The age of Arcida was constrained around 478.6 ± 5 Ma, based on *Glyptarca serrata* (Cope, 1997). Glycymerididae was constrained around 167.7 ± 5 Ma, based on *Trigonarca tumida* (Imlay, 1962). The fossil of *Anadara ferruginea* was used to constrain the age of the subfamily Anadarinae around 138.3 ± 5 Ma (Huber, 2010). Finally, the age of Philobryidae was constrained around 45 ± 11 Ma based on the oldest fossil records for the family (Moore & Teichert, 1969). All priors for fossil ages were drawn from uniform distributions. An uncorrelated exponential model on molecular branch rates was assumed for the relaxed molecular clock. Posterior probabilities were sampled using the MCMC (Markov Chain Monte Carlo) method with four independent chains running for 500,000 iterations, each one containing 534 moves (changes of values in stochastic parameters). Convergence of the posteriors were observed in Tracer version 1.6 (Rambaut *et al.*, 2018). Fossil taxa were then pruned from trees because they were solely used to calibrate node ages, rather than to infer phylogenetic placements. Subsequently, phylogenetic trees were summarized as a maximum clade credibility tree with a burn-in of 10% removed. A lineages-through-time plot was generated in IcyTree (https://icytree.org/).

Character evolution

Mantle margin evolution in Arcida was studied based on morphological data for 64 species from museum collections (Table 1). Specimens were dissected in ethanol and observed under the stereomicroscope for anatomical investigation. Characters were coded and states were assigned to terminals based on observations of the corresponding species. In the absence of data from literature, unobserved species had their states assigned as equivalent to closest relatives (i.e., congeneric species) obtained from collections (supplementary material, Table S1, S2). Characters are related to number and relative size of mantle folds, pigmentation, presence and type of photoreceptor organs, and presence of the mantle nerve (supplementary material, Table S1). Because ethanol often shrinks/distorts tissues during preservation, mantle fold length is a character defined by the relative length of a fold in comparison to another fold, rather than absolute length. Some multistate characters were also coded as binary (see supplementary material, Table S1), as required by the correlation test (Pagel, 1994).

Information on habits of life was compiled from literature for all species included in the phylogenetic analysis (supplementary material, Table S3). Modes of life include: epifaunal (above the substrate, frequently attached to the surface), semi-infaunal (partially buried in soft sediment), and infaunal (buried in soft sediment), with respective modes of byssal attachment, i.e., epibyssate, endobyssate, and abyssate. Additional information was also recovered, such as type of substrate and occurrence relative to depth, varying from shallow (<200 m) to deep waters (>200 m). Subsequently, lifestyles were coded (supplementary material, Table S1, S2) and studied for character evolution as detailed below.

Ancestral state reconstructions (ASR) were conducted under maximum likelihood in Mesquite (Maddison & Maddison, 2018). Two possible models for trait evolution were applied, *i.e.*, the Markov k-state one parameter model (MK1) that assumes equal transition rates and the asymmetrical Markov k-state two parameter model (AsymmMK), in which transition rates can be different. In contrast to the MK1 model, the AsymmMK model allow different rates for "forward" (0→1) and "backward" (1→0) transitions. A likelihood ratio (LR) test was used to verify which model fits the data better (Pagel, 1999, Maddison & Maddison, 2018). Because the two models are nested, the likelihood ratio test follows a chi-square distribution with df=1 (because the AsymmMK model has only one additional parameter than the MK1 model). The reconstructions presented herein follow the statistical decision to reject the null hypothesis (MK1 model) whenever LR>3.84 (critical value for α=0.05, df=1). To evaluate the possible effects of branch supports and alternative topologies in the reconstruction, bootstrap trees were also investigated to inspect the consistency of the reconstructed evolutionary patterns (see Maddison & Maddison, 2018).

Pagel's correlation test was applied in Mesquite (Pagel, 1994; Maddison & Maddison, 2018) to compare the evolution of modes of life and morphological traits, such as photoreceptor organs, mantle folds, and pigmentation. Even though the method has some shortcomings (Maddison & Fitzjohn, 2015), it provides a helpful approach to statistically analyse the evolution of traits by incorporating phylogenetic information. Additionally, tests were conducted considering models representing evolutionary dependence among traits, *i.e.*, when the shift of state in one character likely depends on the state of the second character. Searches were carried out (iterations; n=10) with the p value being estimated from 10,000 repeated simulations. Hypotheses of character correlations were accepted whenever a model with eight-parameters (correlated hypothesis) presented a better fit ($p<0.05$) than a model of evolution with four parameters (uncorrelated hypothesis) (Pagel, 1994; Maddison & Fitzjohn, 2015).

Results

Mantle margin diversity in Arcida

Mantle margin in arcids may comprise four marginal extensions, named mantle folds, identified according to the position relative to the periostracal groove (Fig. 1A, B). They are named, from the outside to the inside: second outer fold (2OF), first outer fold (1OF), middle fold (MF), and inner fold (IF) (Fig. 1B). The second outer fold is a short and delicate projection in a proximal position, present in most Arcida representatives. This structure is usually unpigmented and located close to the region where the pallial muscles are attached to the valve. While this fold is apparent in ark clams and blood cockles, like *Anadara* and *Tegillarca* (Fig. 1L), it seems to be extremely reduced or even absent in smaller species. This is the case of some Philobryidae species (e.g., *Adacnarca*, *Lissarca*, and *Neocardia*) in which the second outer fold was not observed.

The first outer fold is usually well developed in most species, being frequently pigmented and bearing photoreceptor organs. Strong pigmentation is common in epifaunal species, such as *Arca* (Fig. 1D), although pigmentation is also present in some semi-infaunal (e.g., Glycymerididae; Fig. 2E, F) and infaunal species (e.g., some *Anadara* spp.). Photoreceptor organs vary from small eyespots to large compound eyes (Fig. 1, 2). Pigmented eyespots are present in epifaunal Noetiidae, such as *Arcopsis* (Fig. 2B), *Didimacar*, and *Stryarca*, most Arcidae taxa (Fig. 1H), except *Trisidos* (infaunal) and *Bathyarca* (infaunal; deep-sea), and some Philobryidae, including *Lissarca notorcardensis* and *Neocardia* sp. (Fig. 2K). These eyespots are frequently restricted to the anterodorsal region. Compound eyes are larger, multifaceted structures, occurring on the posterior region of *Acar*, *Arca*, *Cucullaea* (Fig. 1C, D, F), Glycymerididae (Fig. 2E, F), and some *Barbatia* species (Fig. 1E, G).

The middle mantle fold, when present, represents a reduced projection, shorter than the first outer fold (Fig. 1E). No photoreceptor or tentacular structures are associated with this projection. The middle fold is absent in the genera *Arca*, *Cucullaea*, and *Trisidos* (Fig. 1C, D, F, N). The mantle margin also lacks a middle fold in Glycymerididae, Philobryidae, and infaunal Noetiidae (e.g., *Eontia* and *Noetia*) (Fig. 2).

The inner mantle fold is an enlarged, muscular projection in most arcid taxa, usually longer and robust posteriorly. In the Cucullaeidae, Glycymerididae, Limopsidae, Philobryidae, and the genus *Arca*, the inner mantle fold is about the length of the first outer fold or slightly longer (Figs. 1D, 2G-M). In contrast, the inner fold is about twice the length of the first outer fold in Noetiidae, *Barbatia*, and *Acar* (Figs. 1E, G). A massive enlargement of the inner fold is observed in some *Barbatia* species and in numerous infaunal species, such as *Trisidos*, *Anadara*, *Tegillarca*, *Eontia*, and *Noetia* (Figs. 1I-N). A posterior flap, formed by the inner fold, is a long projection found in *Bathyarca* species (Fig. 1M).

The mantle margin in arcids exhibits different levels of variation among taxa. For example, fold number and relative lengths are very uniform within the Anadarinae (Fig. 1J-L), but highly variable within *Barbatia* (Fig. 1E, G-I). Within Noetiidae, mantle organization is also variable (Fig. 2A-D), while in Glycymerididae it is more uniform (Fig. 2E, F). In contrast, the Limopsidae (Fig. 2G-I) and Philobryidae (Fig. 2J-M) have a less complex and miniaturized mantle margin, usually devoid of photoreceptor organs, pigmentation or enlarged folds.

Phylogenetic hypotheses

The maximum likelihood tree of the Arcida corroborates the monophyly of the clade, as well as the monophyly of all families, except for Arcidae, which is split into five branches (Fig. 3). Although some internal nodes show low bootstrap values, higher support was obtained for some relationships among families and genera (e.g., *Arca*, Anadarinae, Glycymerididae, Limopsidae). The remaining Pteriomorphia were recovered as the sister-group of Arcida.

Arcidae is polyphyletic in our analysis, with *Arca* and *Acar* descending from an early branch of the order. All Anadarinae species are nested together, being sister-group to a pair of *Barbatia* species (*B. candida* and *B. lacerata*). Interestingly, *Barbatia* species are scattered across the phylogeny, suggesting separate lineages taxonomically included under the same name. Noetiidae is a monophyletic family, although *Adacnarca nitens*, formally a philobryid, seems to also be included in this clade. A close relationship between Limopsidae and Philobryidae was recovered, with Glycymerididae as the sister-group. The three former families were recovered as the sister-group of (*Cucullaea* + *Bathyarca*).

A similar topology was recovered for the time-calibrated phylogeny (Fig. 4). Diversification times were estimated for the major lineages with the 95% highest posterior density interval (HPD): Arcida, 341.3 Ma (95% HPD 261.2–424.1 Ma); Glycymerididae, 194.6 Ma (95% HPD 112.1–278.3 Ma); Anadarinae, 190.5 Ma (95% HPD 124–256.7 Ma); Limopsoidea, 187.7 Ma (95% HPD 113.4–259.3 Ma); Noetiidae, 175.5 Ma (95% HPD 96.6–248.1 Ma); Philobryidae, 143 Ma (95% HPD 77.1–215.9 Ma); and Limopsidae, 110.4 Ma (95% HPD 37.8–195.1 Ma). A lineage-through-time plot also shows a major diversification of Arcida lineages during the Mesozoic (Fig. 4).

Mantle margin evolution

The history of changes in the mantle margin was reconstructed based on key traits. A second outer fold has arisen in the origin of the Arcida clade, and likely lost in Limopsidae and Philobryidae lineages (data not shown). Intense mantle pigmentation was acquired multiple times, *i.e.* in the origin of Glycymerididae, *Arca* + *Acar*, *Barbatia barbata* + *B. cancellaria* + *B. fusca*, and some lineages within Anadarinae (supplementary material, Fig. S1). The ancestor of Arcida had a reduced middle fold, i.e., shorter than the first outer fold (Fig. 5), which is a striking contrast to the remaining Pteriomorphia, in which the middle fold is long and usually bears tentacles and photoreceptor organs. While most arcids share a reduced middle fold, the complete loss of this projection occurred at least ten times (Fig. 5). Photoreceptor organs were reconstructed to be present in the mantle margin of the Arcida's ancestor. More specifically, the presence of pigmented eyespots represents a plesiomorphy for all arcid taxa, with secondary losses for many infaunal lineages, such as *Eontia*, *Limopsis*, and *Trisidos* (Fig. 6A). Similarly, compound eyes were likely present in the Arcida's ancestor, which were subsequently lost in four separate lineages: Limopsoidea, *Bathyarca*, Anadarinae+(*Barbatia candida*+*B. lacerata*), and a clade formed by Noetiidae with some *Barbatia* and *Trisidus* species (supplementary material, Fig. S2).

The inner fold is commonly longer than the other mantle folds in most bivalves, but in Arcida this trait displays significant variation. The inner fold is reconstructed to be about the length of the first outer fold, or only slightly longer, in the origin of the order (Fig. 7A). The enlargement of this fold, forming a long projection about twice the length of the first outer fold, occurred in the *Acar*'s ancestor and in the ancestor of a large clade including Noetiidae, Anadarinae, and *Barbatia* species (Fig. 7A). Another change in state is represented by a very enlarged inner fold, much longer than first outer fold, forming extensible curtains and flaps. This transition occurred in different clades, e.g., *Trisidos*, *Eontia*, *Bathyarca*, and Anadarinae + *Barbatia*, most of them including infaunal bivalves (Fig. 7B).

Association between mantle margin morphology and lifestyles

The reconstruction of modes of life suggests that the ancestor of Arcida was likely an epifaunal bivalve, possibly attached to rocks and hard substrate by byssus (Fig. 6B, supplementary Table S3). Soft sediments, such as mud and sand, were later independently occupied by different groups. The semi-infaunal/infaunal lifestyle was secondarily adopted four times during Arcida evolution during the Mesozoic (Fig.4, 6B), by lineages originating Anadarinae, *Trisidos*, *Eontia* (infaunal noetiids), and the ancestor of all Limopsoidea + Glycymerididae + (*Bathyarca* + Cucullaeidae). Among infaunal lineages, a shift to epifaunal lifestyle has occurred in the origin of Philobryidae (Fig. 6B), animals that are frequently byssate on other organisms, such as algae.

Correlation tests were applied when mantle traits seemed to be associated with particular lifestyles. For instance, pigmentation on the first outer fold is common in epifaunal bivalves. Tested hypotheses of evolutionary correlation are shown in Table 2. Pigmentation, which is typical for epifaunal bivalves, is not statistically correlated to lifestyle (Table 2). Pigmented eyespots, however, had a statistically significant correlation to lifestyle (Table 2). Ancestral state reconstructions of eyespots and lifestyles suggest that this correlation is associated with the adoption of infaunal habits and loss of pigmented eyespots (Fig. 6). Inner fold enlargement is also correlated to mode of life, the results suggesting that the evolutionary shift to infaunal habit was more likely when the inner fold became much longer than the first outer fold (Table 2).

Discussion

Phylogenetic relationships and divergence times

Arcida is a well-supported, monophyletic group (see also Bieler *et al.*, 2014; Feng *et al.*, 2015; Combosch & Giribet, 2016). All families were recovered monophyletic, with the exceptions of a polyphyletic Arcidae and the placement of the philobryid *Adacnarca nitens* within Noetiidae. While a previous analysis found support to separate Arcoidea from Limopsoidea (Combosch & Giribet, 2016), our results indicate Arcoidea as non-monophyletic. This is consequence of an early branch giving rise to *Acar* and *Arca*, while Limopsoidea is nested within the remaining Arcoidea. Therefore, the Limopsoidea would have an origin from within the Arcoidea, a hypothesis not supported by previous topologies (Combosch & Giribet, 2016), but already suggested elsewhere (Jackson *et al.*, 2015). Our topology is consistent with the view that Limopsidae and Philobryidae share an exclusive, common history based on similar development of hinge and alivincular ligament type (Malchus & Warén, 2005; Oliver & Holmes, 2006).

The taxonomic position of Glycymerididae has always been controversial and our data supports this family within Arcoidea, as also suggested by Combosch & Giribet (2016). In contrast to their results, however, the Glycymerididae is the sister group of Limopsoidea in our analysis, forming a clade closely related to *Cucullaea* and *Bathyarca*. The Glycymerididae was previously thought to have originated from the Cucullaeidae based on the duplivincular ligament and other shell characters observed in fossil species (Nicol, 1950). Our results do not corroborate this view, but their morphological similarity is supported by the close relationship between these families.

Arcidae is not monophyletic in our analyses, which is consistent with previous studies (Marko, 2002; Matsumoto, 2003; Feng *et al.*, 2015; Combosch & Giribet, 2016). For instance, the genus *Barbatia* is polyphyletic, and thus in great need of taxonomic revisions. Similarly to previous findings (Combosch & Giribet, 2016), some *Barbatia* species, such as *B. candida* and *B. lacerata*, form the sister group of Anadarinae, while others, such as *B. virescens*, are close to *Trisidos* and Noetiidae.

The oldest fossils of Arcida, i.e. *Glyptarca serrata*, date back to the Ordovician (~480 Ma) (Cope, 1997). According to our analysis, the arcid divergence occurred in late Cambrian (~488 Ma) and the crown group of Arcida had a Carboniferous origin, around 341 Ma. Our time-calibrated phylogeny agrees with the fossil record (Thomas, 1978a; Oliver & Holmes, 2006), suggesting most diversification of Arcida occurred during the Mesozoic, including the origin of most modern families, i.e., Cucullaeidae, Glycymerididae, Limopsidae, and Philobryidae. The convergent transitions to semi-infaunal or infaunal habits by different lineages, such as noetiids, Anadarinae, Cucullaeidae, Glycymerididae, and Limopsidae, may have contributed to the diversification of Arcida, which is consistent with the Cretaceous fossil record (Thomas, 1978b; Thomas *et al.*, 2000; Oliver & Holmes, 2006; Combosch & Giribet, 2016). The adoption of an infaunal lifestyle in bivalves is regarded as one of the most important strategies to avoid predation by a diversity of duraphagous predators during the long-lasting ecological arms race of the so-called Mesozoic Marine Revolution (Stanley, 1968; Vermeij, 1977). Our results provide, therefore, further evidence for the Mesozoic infaunalization of bivalves.

Evolution of mantle traits and lifestyle

The second outer mantle fold is an exclusive feature of Arcida, shared by most of its descendants (see also Waller, 1980). Photoreceptor organs on the first outer fold are also distinctive traits of Arcida, and they are present mainly in epifaunal species inhabiting shallow waters (Waller, 1980; Morton & Peharda, 2008; Morton & Puljas, 2015; Audino & Marian, 2018; present study). Our data support the correlated evolution of photoreceptor organs and mode of life, as previously suggested based on morphological studies alone (Audino & Marian, 2018).

The Arcida's ancestor had pigmented eyespots and posterior compound eyes that were lost in numerous lineages (Fig. 6, S2). These findings suggest an important role of light-guided behaviors in ancestral ark clams living on the substrate, possibly related to predator detection and posture control (Nilsson, 1994). A single origin of compound eyes is in accordance with the anatomical similarity of these organs in the distinct arcidan lineages that were studied so far, such as Glycymerididae, the genera *Arca* and *Acar*, and some *Barbatia* species (Waller, 1980; Morton & Puljas, 2015, Audino & Marian, 2018). Additionally, the loss of photoreceptor organs also provides important insights into the evolution of ark clams. Infaunal lineages frequently lost photoreceptor organs present in their epifaunal ancestor (Fig. 6, S2), which can be explained either by a condition of relaxed selection under the infaunal condition or a positive selective pressure for eye reduction.

Relaxed selection can be defined as the elimination or reduction, by means of environmental changes, of a selective force that was important for the maintenance of a particular trait (Lahti *et al.*, 2009). This is an evolutionary process frequently evoked to explain eye and pigment reduction in several groups, including numerous lineages of cave animals (Porter & Crandall, 2003; Wilkens, 2010). Alternatively, other processes can also produce similar patterns. For example, variability in eye size and pigmentation in cave fishes occurs through multiple mechanisms, suggesting different evolutionary forces synergistically driving eye regression via pleiotropy (Protas *et al.*, 2008). Studies of both vertebrate and invertebrate cave lineages have also demonstrated the high energetic costs of maintaining sensory systems, such as eyes, even in dark conditions (Niven 2007; Niven & Laughlin 2008). For example, eye loss in cavefishes may have been driven by selection for regression of neural tissue, which is associated with high metabolic costs (Moran *et al.*, 2015). In cave crabs, eye reduction seems to be most likely driven by strong directional selective regimes in the subterranean environment (Klaus *et al.*, 2013). In the marine infaunal context, our results provide the initial steps to understand the evolutionary trajectory of photoreceptor organs in ark clams. Similar to many intriguing cave lineages' cases (Niven, 2007), further studies are still necessary to clarify if eye loss in infaunal bivalves is produced by selective pressure or by genetic drift when selective pressures for eye maintenance are absent.

The middle fold is a mantle margin projection usually well-developed in most bivalves, frequently bearing associated structures and playing sensorial roles (Yonge, 1983). An opposite condition was observed in most specimens studied herein, in which the middle fold is shorter than the outer and inner folds, corresponding to only a slight projection, when present. A shorter middle fold was also noted in *Limopsis cristata* (Morton, 2013) and *Barbatia* species (Simone & Chichvarkhin, 2004). Our results suggest that this fold was already reduced in the ancestor of Arcida, which is a remarkable difference from other pteriomorphians, which frequently display a long and complex projection (Audino & Marian, 2016). The reduction of the middle fold seems to have been a common phenomenon during Arcida diversification, resulting in the complete loss of this structure in several lineages (Fig. 5). Such evolutionary pattern is unique among bivalves and leaves many unsolved functional questions. One possible explanation was provided by Morton (1982), who suggested that sensorial roles, such as photoreception, were transferred to the first outer fold. In addition, recent anatomical evidence from different arcid species also corroborated this view, indicating that chemo-/mechano-sensorial roles were possibly transferred to the enlarged inner fold (Audino & Marian, 2018).

The hypertrophy of the inner fold in a very extensible organ is observed in many lineages of Arcida (Fig. 7). For example, most semi-infaunal or infaunal arcids, such as some Noetiidae, Anadarinae, *Trisidos*, and *Bathyarca*, have very long inner folds (see also Morton, 1982; Audino & Marian, 2018). In infaunal bivalves of other clades (e.g., Heterodonta), siphons (i.e., long, fused inner folds) are present and allow them to inhabit soft sediments and maintain water circulation through the pallial cavity (Yonge, 1983). In the case of the infaunal *Bathyarca pectunculoides*, the posterior flaps formed by the inner fold are thought to act as functional siphons (Morton, 1982). Accordingly, our phylogenetic and morphological data strongly support the evolution of the inner fold as a functional siphon in arcid lineages, which has possibly facilitated the transition to infaunal lifestyles.

Evolutionary convergence and macroevolution

Ecological shifts shaping morphological evolution are known for many vertebrate groups (e.g., lizards, Mahler *et al.*, 2013; fishes, Davis & Betancur-R, 2017; snakes, Esquerré & Scott Keogh, 2016). While marine invertebrates still lack detailed information about ecomorphological evolution, recent progress has been achieved using different clades as models. In cephalopods, for example, several morphological traits represent evolutionary convergences and possible adaptive features associated with benthic or pelagic environments (Lindgren *et al.*, 2012). While bivalves have traditionally being considered classic examples of convergent evolution associated with life-habits in the marine benthos (e.g., Stanley, 1972), even in Invertebrate Zoology textbooks (e.g., Ruppert *et al.*, 2004), these adaptive hypotheses have rarely been tested under an explicit phylogenetic approach. In this context, important progresses were recently obtained for Pectinidae (Alejandrino *et al.*, 2011; Serb *et al.*, 2017) and Galeommatoidea (Li *et al.*, 2016).

The Arcida have been consistently regarded as an example of adaptive radiation, with their homoplastic shell characters adapted to infaunal and epifaunal modes of life (Stanley, 1968, 1972; Thomas, 1976, 1978a). Our study provides, for the first time, phylogenetic-based evidence for correlated evolution between morphology of soft parts and lifestyle transitions in arcids. In addition, evolutionary convergence seems a recurrent pattern, including independent losses of eyespots, compound eyes, pigmentation and middle fold, as well as independent enlargements of the inner fold. Our results suggest that predation pressure was important in the evolution of Arcida, mainly during the Mesozoic. Pigmented eyespots and compound eyes may aid in predator recognition in epifaunal bivalves (Nilsson, 1994), while the infaunal habit itself, facilitated by enlarged mantle curtains, may have been a response to predation pressure (Bush & Bambach, 2011). The dramatic increase of infaunal lineages in the marine benthos suggests a successful trend to survive the intensification of predation during the Mesozoic Marine Revolution (Stanely, 1968, 1972; Vermeij, 1977). In addition to the extensive fossil information for hard parts, we were able to contribute to this hypothesis based on the soft parts of extant lineages of arcids in an integrative approach. Altogether, our results demonstrate evolutionary associations between ecology and morphology during the diversification of bivalve lineages across different benthic lifestyles.

Acknowledgments

The authors acknowledge the grants 2015/09519-4 and 2017/01365-3, São Paulo Research Foundation (FAPESP). This study was financed in part by the Coordenação de Aperfeiçoamento de Pessoal de Nível Superior - Brasil (CAPES) - Finance Code 001. This study is part of the first author's Doctorate's thesis through the Graduate Program in Zoology of the Institute of Biosciences (University of São Paulo). The authors thank the following institutions that provided materials for the development of this study: Museum of Comparative Zoology (MCZ), Museum of Zoology "Prof. Adão José Cardoso" of the University of Campinas (ZUEC), Museum of Zoology of the University of São Paulo (MZSP), Santa Barbara Museum of Natural History (SBMNH), and Smithsonian National Museum of Natural History (USNM). We also thank two anonymous reviewers for their helpful comments. This is a contribution of NP-BioMar (Research Center for Marine Biodiversity – USP).

References

Alejandrino A, Puslednik L, Serb JM. 2011. Convergent and parallel evolution in life habit of the scallops (Bivalvia: Pectinidae). *BMC Evolutionary Biology* 11: 164.

Audino JA, Marian JEAR. 2016. On the evolutionary significance of the mantle margin in pteriomorphian bivalves. *American Malacological Bulletin* 34: 148–159.

Audino JA, Marian JEAR. 2018. Comparative and functional anatomy of the mantle margin in ark clams and their relatives (Bivalvia: Arcoidea) supports association between morphology and life habits. *Journal of Zoology* 305(3): 149–162.

Bieler R, Mikkelsen PM, Collins TM, Glover EA, González VL, Graf DL, Harper EM, Healy J, Kawauchi GY, Sharma PP, Staubach S, Strong EE, Taylor JD, Tëmkin I, Zardus JD, Clark S, Gusmán A, McIntyre E, Sharp P, Giribet G. 2014. Investigating the Bivalve Tree of Life - An exemplar-based approach combining molecular and novel morphological characters. *Invertebrate Systematics* 28: 32–115.

Bush AM, Bambach RK. 2011. Paleoecologic megatrends in marine metazoa. *Annual Review of Earth and Planetary Sciences* 39: 241–269.

Carter JG, Altaba CR, Anderson LC, Araujo R, Biakov AS, Bogan AE, Campbell DC, Campbell M, Jin-hua C, Cope JCW, Dijkstra HH, Zong-jie F, Gardner RN, Gavrilova VA, Goncharova IA, Harries PJ, Hartman JH, Hautmann M, Hoeh WR, Hylleberg J, Johnston P, Kirkendale L, Kleemann K, Koppka J, Machado D, Malchus N, Márquez-aliaga A, Masse J pierre, Mcroberts CA, Peter U, Mitchell S, Nevesskaja LA, Özer S, Jr JP, Polubotko I V, Pons M, Popov S, Sánchez T, Sartori AF, Scott RW, Sey II, Javier H, Silantiev V V, Skelton PW, Steuber T, Waterhouse JB, Lynn G, Yancey T, Carter JG, Altaba CR, Anderson LC, Araujo R, Biakov AS, Bogan AE, Campbell DC, Campbell M, Jin-hua C, Cope JCW, Delvene G, Dijkstra HH, Gardner RN, Gavrilova VA, Goncharova IA, Harries PJ, Hartman JH, Hoeh WR, Hylleberg J, Bao-yu J, Johnston P, Kirkendale L, Kleemann K, Middelfart PU, Mitchell S, Nevesskaja LA, Özer S, Pojeta J, Polubotko I V, Silantiev V V, Skelton PW, Steuber T, Waterhouse JB, Wingard GL, Yancey T, Harries PJ, Skelton P. 2011. A synoptical classification of the Bivalvia (Mollusca). *Paleontological Contributions* 4: 1–47.

Combosch DJ, Giribet G. 2016. Clarifying phylogenetic relationships and the evolutionary history of the bivalve order Arcida (Mollusca: Bivalvia: Pteriomorphia). *Molecular Phylogenetics and Evolution* 94: 298–312.

Cope JCW. 1997. The early phylogeny of the class Bivalvia. *Palaeontology* 40: 713–746.

Cope JCW. 2000. A new look at early bivalve phylogeny. *Geological Society, London, Special Publications* 177: 81–95.

Davis AM, Betancur-R R. 2017. Widespread ecomorphological convergence in multiple fish families spanning the marine–freshwater interface. *Proceedings of the Royal Society B:*

Biological Sciences 284: 20170565.

Esquerré D, Scott Keogh J. 2016. Parallel selective pressures drive convergent diversification of phenotypes in pythons and boas. *Ecology Letters* 19(7): 800–809.

Felsenstein J. 1985. Confidence limits on phylogenies: an approach using the bootstrap. *Evolution* 39: 783–791.

Feng Y, Li Q, Kong L. 2015. Molecular phylogeny of Arcoidea with emphasis on Arcidae species (Bivalvia: Pteriomorphia) along the coast of China: Challenges to current classification of arcoids. *Molecular Phylogenetics and Evolution* 85: 189–196.

Giribet G, Wheeler W. 2002. On bivalve phylogeny: a high-level analysis of the Bivalvia (Mollusca) based on combined morphology and DNA sequence data. *Invertebrate Biology* 121: 271–324.

Gould SJ, Vrba ES. 1982. Exaptation—a missing term in the science of form. *Paleobiology* 8(1): 4–15.

Harvey PH, Pagel MD. 1991. *The comparative method in evolutionary biology*. Oxford: Oxford University Press.

Heath TA, Huelsenbeck JP, Stadler T. 2014. The fossilized birth--death process for coherent calibration of divergence-time estimates. *Proceedings of the National Academy of Sciences* 111: E2957–E2966.

Höhna S, Landis MJ, Heath TA, Boussau B, Lartillot N, Moore BR, Huelsenbeck JP, Ronquist F. 2016. RevBayes: Bayesian phylogenetic inference using graphical models and an interactive model-specification language. *Systematic Biology* 65: 726–736.

Huber M. 2010. *Compendium of Bivalves*. Hackenheim: ConchBooks.

Imlay RW. 1962. *Jurassic (Bathonian or early Callovian) ammonites from Alaska and Montana*. US Government Printing Office.

Jackson JA, Linse K, Whittle R, Griffiths HJ. 2015. The evolutionary origins of the southern ocean philobryid bivalves: Hidden biodiversity, ancient persistence. *PLoS ONE* 10(4): e0121198.

Kalyaanamoorthy S, Minh BQ, Wong TKF, von Haeseler A, Jermiin LS. 2017. ModelFinder: fast model selection for accurate phylogenetic estimates. *Nature Methods* 14: 587.

Katoh K, Standley DM. 2013. MAFFT multiple sequence alignment software version 7: improvements in performance and usability. *Molecular Biology and Evolution* 30: 772–780.

Klaus S, Mendoza JCE, Liew JH, Plath M, Meier R, Yeo DCJ. 2013. Rapid evolution of troglomorphic characters suggests selection rather than neutral mutation as a driver of eye reduction in cave crabs. *Biology Letters* 9(2): 20121098.

Lahti DC, Johnson NA, Ajie BC, Otto SP, Hendry AP, Blumstein DT, Coss RG, Donohue K, Foster SA. 2009. Relaxed selection in the wild. *Trends in Ecology and Evolution* 24: 487–496.

Li J, Ó Foighil D, Strong EE. 2016. Commensal associations and benthic habitats shape macroevolution of the bivalve clade Galeommatoidea. *Proceedings of the Royal Society B: Biological Sciences* 283: 20161006.

Lindgren AR, Pankey MS, Hochberg FG, Oakley TH. 2012. A multi-gene phylogeny of Cephalopoda supports convergent morphological evolution in association with multiple habitat shifts in the marine environment. *BMC Evolutionary Biology* 12: 129.

Losos JB. 2011. Convergence, adaptation, and constraint. *Evolution* 65: 1827–1840.

Losos JB, Mahler DL. 2010. Adaptive radiation: The interaction of ecological opportunity, adaptation, and speciation. In: Bell MA, Futuyma DJ, Eanes WF, Levinton JS, eds. *Evolution since Darwin: the first 150 years*. Sanderland: Sinauer Associates, 381–420.

Maddison WPM, Fitzjohn RG. 2015. The unsolved challenge to phylogenetic correlation tests for categorical characters. *Systematic Biology* 64: 127–136.

Maddison WP, Maddison DR. 2018. Mesquite: a modular system for evolutionary analysis. Version 3.51 http://www.mesquiteproject.org

Mahler DL, Ingram T, Revell LJ, Losos JB. 2013. Exceptional convergence on the macroevolutionary landscape in island lizard radiations. *Science* 341(6143): 292–295.

Mahler DL, Weber MG, Wagner CE, Ingram T. 2017. Pattern and process in the comparative study of convergent evolution. *The American Naturalist* 190: S13–S28.

Malchus N, Warén A. 2005. Shell and hinge morphology of juvenile *Limopsis* (Bivalvia: Arcoida) - Implications for limopsid evolution. *Marine Biology Research* 1(5): 350–364.

Malkowsky Y, Götze MC. 2014. Impact of habitat and life trait on character evolution of pallial eyes in Pectinidae (Mollusca: Bivalvia). *Organisms Diversity & Evolution* 14(2): 173–185.

Marko PB. 2002. Fossil calibration of molecular clocks and the divergence times of geminate species pairs separated by the Isthmus of Panama. *Molecular Biology and Evolution* 19: 2005–2021.

Matsumoto M. 2003. Phylogenetic analysis of the subclass Pteriomorphia (Bivalvia) from mtDNA COI sequences. *Molecular Phylogenetics and Evolution* 27: 429–440.

Moore RC, Teichert C. 1969. *Treatise on Invertebrate Paleontology: Pt. N Mollusca 6, Bivalvia*. Geological Society of America.

Morton B. 1982. Functional morphology of *Bathyarca pectunculoides* (Bivalvia: Arcacea) from a deep Norwegian fjord with a discussion of the mantle margin in the Arcoida. *Sarsia* 67: 269–282.

Morton B. 2013. The functional morphology of the abyssal *Limopsis cristata* (Arcoida: Limopsidae) with a discussion on the evolution of the more advanced bivalve foot. *Acta Zoologica* 94: 74–85.

Morton B, Peharda M. 2008. The biology and functional morphology of *Arca noae* (Bivalvia:

Arcidae) from the Adriatic Sea, Croatia, with a discussion on the evolution of the bivalve mantle margin. *Acta Zoologica* 89: 19–28.

Morton B, Prezant RS, Wilson B. 1998. Class Bivalvia. In: Beesley PL, Ross GJB, Wells A, eds. *Mollusca: The southern synthesis. Fauna of Australia. Vol. 5*. Melbourne: CSIRO Publishing, 195–234.

Morton B, Puljas S. 2015. The ectopic compound ommatidium-like pallial eyes of three species of Mediterranean (Adriatic Sea) *Glycymeris* (Bivalvia: Arcoida). Decreasing visual acuity with increasing depth? *Acta Zoologica* 474: 464–474.

Nguyen LT, Schmidt HA, von Haeseler A, Minh BQ. 2014. IQ-TREE: a fast and effective stochastic algorithm for estimating maximum-likelihood phylogenies. *Molecular Biology and Evolution* 32: 268–274.

Nicol D. 1950. Origin of the pelecypod family Glycymeridae. *Journal of Paleontology* 24: 89–98.

Nilsson DE. 1994. Eyes as optical alarm systems in fan worms and ark clams. *Philosophical Transactions of the Royal Society B: Biological Sciences* 346(1316): 195–212.

Oliver PG, Holmes AM. 2006. The Arcoidea (Mollusca: Bivalvia): A review of the current phenetic-based systematics. *Zoological Journal of the Linnean Society* 148: 237–251.

Pagel M. 1994. Detecting correlated evolution on phylogenies: a general method for the comparative analysis of discrete characters. *Proceedings of the Royal Society B-Biological Sciences* 255: 37–45.

Pagel M. 1999. The maximum likelihood approach to reconstructing ancestral character states of discrete characters on phylogenies. *Systematic Biology* 48(3): 612–622.

Pojeta J, Runnegar B, Kriz J. 1973. *Fordilla troyensis* Barrande: the oldest known pelecypod. *Science* 180: 866–868.

Porter ML, Crandall KA. 2003. Lost along the way: The significance of evolution in reverse.

Trends in Ecology and Evolution 18: 541–547.

Protas M, Tabansky I, Conrad M, Gross JB, Vidal O, Tabin CJ, Borowsky R. 2008. Multi-trait evolution in a cave fish, *Astyanax mexicanus*. *Evolution & Development* 10: 196–209.

Rambaut A, Drummond AJ, Xie D, Baele G, Suchard MA. 2018. Posterior summarisation in Bayesian phylogenetics using Tracer 1.7. *Systematic Biology* syy032

Schluter D. 2000. *The ecology of adaptive radiation*. Oxford: Oxford University Press.

Serb JM, Sherratt E, Alejandrino A, Adams DC. 2017. Phylogenetic convergence and multiple shell shape optima for gliding scallops (Bivalvia: Pectinidae). *Journal of Evolutionary Biology* 30: 1736–1747.

Simone LRL, Chichvarkhin AY. 2004. Comparative morphological study of four species of *Barbatia* occurring on the southern Florida coast (Arcoidea, Arcidae). *Malacologia* 46: 355–379.

Simpson GG. 1953. *The major features of evolution*. New York: Columbia University Press.

Stanley SM. 1968. Post-Paleozoic adaptive radiation of infaunal bivalve molluscs: A consequence of mantle fusion and siphon formation. *Journal of Paleontology* 42: 214–229.

Stanley SM. 1972. Functional morphology and evolution of byssally attached bivalve mollusks. *Journal of Paleontology* 46: 165–212.

Steiner G, Hammer S. 2000. Molecular phylogeny of the Bivalvia inferred from 18S rDNA sequences with particular reference to the Pteriomorphia. *Geological Society, London, Special Publications* 177: 11–29.

Thomas RDK. 1976. Constraints of ligament growth, form and function on evolution in the Arcoida (Mollusca: Bivalvia). *Paleobiology* 2: 64–83.

Thomas RDK. 1978a. Shell form and the ecological range of living and extinct Arcoida. *Paleobiology* 4: 181–194.

Thomas RDK. 1978b. Limits to opportunism in the evolution of the Arcoida (Bivalvia). *Philosophical Transactions of the Royal Society B: Biological Sciences* 284: 335–344.

Thomas RDK, Madzvamuse A, Maini PK, Wathen AJ. 2000. Growth patterns of noetiid ligaments: implications of developmental models for the origin of an evolutionary novelty among arcoid bivalves. *Geological Society, London, Special Publications* 177: 279–289.

Vermeij GJ. 1977. The Mesozoic Marine Revolution: Evidence from snails, predators and grazers. *Journal of Paleontology* 3: 245–25.

Waller TR. 1980. Scanning electron microscopyof shell and mantle in the order Arcoida. *Smithsonian Contributions to Zoology* 313: 1–58.

Wilkens H. 2010. Genes, modules and the evolution of cave fish. *Heredity* 105: 413.

Yonge CM. 1983. Symmetries and the role of the mantle margins in the bivalve Mollusca. *National Wildlife* 16: 1–10.

Figure legends

Figure 1. General organization of the mantle (**A**) and mantle margin (**B**) in Arcida represented by simplified schemes. Mantle margin morphology in Arcidae (C-E, G-N) and Cucullaeidae (F). Posterior mantle region, ventral view. Scale bars = 1mm. The first outer fold can be pigmented (C-G), bearing multiple compound eyes (arrows) and pigmented eyespots (arrowheads). The middle fold is reduced (E) or absent (J). The inner fold is much longer than the other folds, forming a large curtain (I-N) or a posterior flap (M). **C.** *Acar plicata* (USNM 886349). **D.** *Arca noae* (USNM 1086014). **E.** *Barbatia fusca* (SBMNH 349329). **F.** *Cucullaea labiata* (USNM 746883). **G.** *Barbatia barbata* (MCZ 378867). **H.** *Barbatia virescens* (MCZ 378874). **I.** *Barbatia candida* (MZSP 105572). **J.** *Anadara broughtonii* (USNM 802331). **K.** *Anadara ferruginea* (SBMNH 81002). **L.** *Tegillarca granosa* (MCZ 378820). **M.** *Bathyarca corpulenta* (SBMNH 349320). **N.** *Trisidos kiyonoi* (SBMNH 97422). Abbreviations: aa, anterior adductor; if, inner fold; ma, mantle; mf, middle fold; mm, mantle margin; of, outer fold; of-1, first outer fold; of-2, second outer fold; pa, posterior adductor; pe, pigmented eyespots; pg, periostracal groove; sh, shell.

Figure 2. Mantle margin morphology in Noetiidae (A-D), Glycymerididae (E, F), Limopsidae (G-I), and Philobryidae (J-M). Posterior mantle region. Scale bars = 1mm. The first outer fold can bear compound eyes (arrows) and pigmented eyespots (arrowheads). **A.** *Striarca lactea* (USNM 857645). **B.** *Arcopsis solida* (USNM 733218). **C.** *Didimacar tenebrica* (SBMNH 80722). **D.** *Noetia ponderosa* (USNM 803530). **E.** *Tucetona pectinata* (MZSP 91971). **F.** *Glycymeris tenuicostata* (378982). **G.** *Limopsis aurita* (ZUEC-BIV 2248). **H.** *Limopsis lilliei* (MZSP 90647). **I.** *Limopsis marionensis* (USNM 760835). **J.** *Adacnarca nitens* (USNM 886551). **K.** *Lissarca notorcadensis* (MZSP 87826). **L.** *Neocardia sp.* (MCZ 378927). **M.**

Philobrya sublaevis (MZSP 90645). Abbreviations: if, inner fold; ma, mantle; mm, mantle margin; of-1, first outer fold.

Figure 3. Phylogenetic relationships within Arcida based on maximum likelihood analysis of four genes (18S rRNA, 28S rRNA, COI mtDNA, and H3). Asterisks on nodes indicate bootstrap values > 95%. Selected clades are indicated by color groups. Arcidae is the only non-monophyletic family.

Figure 4. Time-calibrated phylogeny of Arcida under Bayesian inference based on four genes (18S rRNA, 28S rRNA, COI mtDNA, and H3) and five fossils used to calibrate internal nodes (red circles). Green values indicate median ages on selected nodes. Grey bars indicate 95% highest posterior density intervals (HPD) for nodes of interest. Posterior probabilities different than 1.0 are indicated on nodes. Color code for clades and taxa is the same used in Figure 3. A lineages-through-time plot is shown at the upper left. After a Cambrian divergence, the crown group of Arcida had an origin around 341 Ma (Carboniferous) and a major diversification during the Mesozoic.

Figure 5. Ancestral state reconstruction of the middle mantle fold in Arcida under maximum likelihood, assuming a single rate for all possible transitions (MK1 model). Pie charts represent the likelihood proportions of reconstructed states; nodes of interest have their charts enlarged. Mantle margin schemes indicate mantle morphology as reconstructed by the analysis. Abbreviations: ce, compound eyes; if, inner fold; ma, mantle; mf, middle fold; of, outer fold; of-1, first outer fold; of-2, second outer fold; pc, pigmented eyespots; sh, shell.

Figure 6. Ancestral state reconstruction of mantle photoreceptor organs (left, AsymmMK model) and mode of life (right, MK1 model) in Arcida under maximum likelihood. Ingroup is indicated by the grey boxes. Pie charts represent the likelihood proportions of reconstructed states; nodes of interest have their charts enlarged. The Arcida's ancestor is recovered as an epifaunal animal with simple eyespots on the mantle. Most subsequent losses of eyespots (red left arrows) are apparently associated with transitions to semi-infaunal/infaunal habits (red right arrows). Abbreviations: if, inner fold; ma, mantle; mf, middle fold; of, outer fold; of-1, first outer fold; pc, pigmented eyespots; sh, shell.

Figure 7. Ancestral state reconstruction of inner fold length (left) and mode of life (right) in Arcida under maximum likelihood, assuming a single rate for all possible transitions (MK1 model). Ingroup is indicated by the grey boxes. Pie charts represent the likelihood proportions of reconstructed states; nodes of interest have their charts enlarged. The inner mantle fold becomes much longer than the others in numerous lineages (left arrows), which is apparently associated with transitions to semi-infaunal/infaunal habits (right arrows). Abbreviations: if, inner fold; ma, mantle; of-1, first outer fold; of-2, second outer fold; sh, shell.

Supplementary material legends

Tables

Table S1. Characters and states used to study mantle margin traits and lifestyles in Arcida.

Table S2. Matrix of mantle margin traits and taxa used in the analyses.

Table S3. Lifestyle compilation of ark clams and relatives (Arcida) according to mode of attachment on the substrate and position.

Figures

Figure S1. Ancestral state reconstruction of pigmentation on the first outer mantle fold in Arcida under maximum likelihood, assuming a single rate for all possible transitions (MK1 model). Pie charts represent the likelihood proportions of reconstructed states. Pigmentation has evolved multiple times in different lineages of epifaunal and infaunal arcids.

Figure S2. Ancestral state reconstruction of compound eyes on the first outer mantle fold in Arcida under maximum likelihood, allowing for a different rate for transitions (AsymmMK model). Pie charts represent the likelihood proportions of reconstructed states. Compound eyes have a single origin in the ancestor of Arcida with subsequent losses in at least four lineages. Abbreviations: ce, compound eyes; if, inner fold; ma, mantle; mf, middle fold; of-1, first outer fold; of-2, second outer fold; sh, shell.

Table 1. Taxa included in the phylogenetic and morphological analyses. Nucleotide sequences were obtained in *GenBank* database; accession numbers are listed. Morphological investigation was conducted with taxa included in the phylogenetic study (when possible) and additional species; catalogue numbers are indicated. Abbreviations: Museum of Comparative Zoology (MCZ), Museum of Zoology “Prof. Adão José Cardoso” of the University of Campinas (ZUECBIV), Museum of Zoology of the University of São Paulo (MZSP), Smithsonian National Museum of Natural History (USNM), Santa Barbara Museum of Natural History (SBMNH).

Taxa	**Reference**	**18S rRNA**	**28S rRNA**	**COI mtDNA**	**Histone H3**	**Collections**
Arcidae						
Acar dominguensis	(Lamarck, 1819)			FJ480593	KT757861	MZSP118292
Acar gradata	(Broderip & Sowerby I, 1829)					USNM796185
Acar plicata	(Dillwyn, 1817)	AJ389630	AJ307533	FJ480453	AF416856	MZSP115322
Anadara antiquata	(Linnaeus, 1758)	JN974491	JN974542	HQ258850	JN974592	MZSP99848
Anadara baughmani	Hertlein, 1951					USNM803522
Anadara broughtonii	(Schrenck, 1867)	JN974489	JN974541	HQ258847	JN974590	USNM802331
Anadara chemnitzii	(Philippi, 1851)					MZSP43259, ZUECBIV4870
Anadara cornea	(Reeve, 1844)	JN974499	DQ343860	HQ258856	JN974600	
Anadara crebricostata	(Reeve, 1844)	JN974495	JN974547	HQ258859	JN974596	
Anadara ferruginea	(Reeve, 1944)					SBMNH81002
Anadara floridana	(Conrad, 1869)					USNM847847
Anadara globosa	(Reeve, 1844)	JN974484	JN974535	HQ258861	JN974584	
Anadara grandis	(Broderip & Sowerby I, 1829)					USNM803487
Anadara gubernaculum	(Reeve, 1844)	JN974493	JN974544	HQ258857	JN974594	

Taxa	**Reference**	**18S rRNA**	**28S rRNA**	**COI mtDNA**	**Histone H3**	**Collections**
Anadara inaequivalvis	(Bruguiere, 1789)	JN974497	JN974548	AB076937	JN974598	MZSP55060
Anadara notabilis	(Röding, 1798)	KT757768	KT757816	AF416828	KT757863	MZSP84987, MZSP84886
Anadara obesa	(G. B. Sowerby I, 1833)					MCZ337676
Anadara pilula	(Reeve, 1843)	JN974507	JN974558	HQ258862	JN974608	
Anadara subcrenata	(Lischle, 1869)	JN974501	DQ343861	HQ258851	JN974602	
Anadara transversa	(Say, 1822)					USNM801135, MCZ359001
Anadara trapezia	(Deshayes, 1839)	KT757770	KT757817	KX713443	KT757865	SBMNH10187
Anadara vellicata	(Reeve, 1844)	JN974487	JN974539	HQ258848	JN974588	
Arca imbricata	Bruguière, 1789	AY654986	KT757820	AF253494	AY654989	MZSP95208, MZSP109869
Arca navicularis	Bruguière, 1789	JN974517	KT757821	HQ258822	JN974618	USNM719071, MCZ378833
Arca noae	Linnaeus, 1758	KC429325	KT757822	KC429090	KC429160	USNM1086014
Arca patriarchalis	Röding, 1798	JN974527	JN974576		JN974627	MZSP99765
Arca ventricosa	(Lamarck, 1819)			AB076935	AF416854	MZSP55027
Arca zebra	(Swainson, 1833)	KT757776	KT757824		AF416864	MZSP101688
Barbatia amygdalumtostum	(Röding, 1798)	JN974526	JN974575		JN974626	SBMNH349329, USNM847011
Barbatia barbata	(Linnaeus, 1758)	KC429326	KT757825	KC429091	KC429161	MCZ378867
Barbatia cancellaria	(Lamarck, 1819)	KT757779	KT757827			MZSP32336, MZSP48857

Taxa	Reference	18S rRNA	28S rRNA	COI mtDNA	Histone H3	Collections
Barbatia candida	(Helbling, 1779)	KT757784	KT757831	AF253487	AF416849	MZSP105572, ZUECBIV1407
Barbatia lacerata	(Bruguière, 1789)	JN974509	JN974560	HQ258826	JN974610	
Barbatia lima	(Reeve, 1844)	JN974511	JN974563	HQ258837	JN974612	MZSP71135
Barbatia virescens	(Reeve, 1844)	JN974524	KT757835	HQ258840	JN974624	MZSP71367, MCZ378874
Bathyarca corpulenta	(E A Smith, 1885)					SBMNH349320
Bathyarca glomerula	(Dall, 1881)	KT757790	KT757837		KT757880	
Bathyarca pectunculoides	(Scacchi, 1835)					MCZ348402
Bentharca asperula	(Dall, 1881)					MCZ348399
Lunarca ovalis	(Bruguière, 1789)			GQ166571	AF416844	MZSP84823, USNM803532
Tegillarca granosa	(Linnaeus, 1758)	JN974505	KT757857	HQ258867	JN974606	MZSP55596, MCZ378820
Tegillarca nodifera	(Martens, 1860)	JN974503	JN974554	HQ258869	JN974604	
Trisidos kiyonoi	(Makiyama, 1931)	JN974522	JN974571	HQ258846	JN974622	SBMNH97422, SBMNH97423
Trisidos tortuosa	(Linnaeus, 1758)	KT757811	KT757858		KT757899	
Cucullaeidae						
Cucullaea labiata	(Lightfoot, 1786)	JN974513	JN974565	KJ774477	JN974614	USNM746883
Noetiidae						
Arcopsis adamsi	(Dall, 1886)	KC429327	KC429419	KC429092	KC429162	MZSP19724, ZUECBIV1153

Taxa	**Reference**	**18S rRNA**	**28S rRNA**	**COI mtDNA**	**Histone H3**	**Collections**
Didimacar tenebrica	(Reeve, 1844)	JN974515	JN974566	HQ258870	JN974616	SBMNH80722
Eontia ponderosa	(Say, 1822)	KT757793	KT757840	AF416834	AF416860	SBMNH235066, USNM803530
Sheldonella bisulcata	(Lamarck, 1819)					MZSP26911
Striarca lactea	(Linnaeus, 1758)	AF120531	KT757855	AF120646		USNM857645, MCZ379156
Striarca symmetrica	(Reeve, 1844)					MZSP55574
Glycymerididae						
Glycymeris decussata	(Linnaeus, 1758)					MZSP91966
Glycymeris gigantea	(Reeve, 1843)	KT757794	KT757841		KT757883	MCZ 378989
Glycymeris glycymeris	(Linnaeus, 1758)	KC429328	KC429421	KC429093	KC429163	USNM794960
Glycymeris holoserica	(Reeve, 1843)	KT757796	KT757843		KT757885	MCZ378984
Glycymeris longior	(G B Sowerby, 1833)					MZSP91201, ZUECBIV78
Glycymeris nummaria	(Linnaeus, 1758)	KT757798	KT757845	KX785178	KT757887	MCZ378985
Glycymeris septentrionalis	(Middendorff, 1849)	KT757799	KT757846	KF643645	KT757888	
Glycymeris tenuicostata	(Reeve, 1843)	KT757800	KT757847		KT757889	MCZ378982
Glycymeris undata	(Linnaeus, 1758)					MZSP91983
Tucetona pectinata	(Gmelin, 1791)	KT757812	KT757859	KX713507	KT757900	MZSP91971, ZUECBIV2198
Limopsidae						
Limopsis aurita	(Brocchi, 1814)					ZUECBIV2248, MCZ348438

Taxa	Reference	18S rRNA	28S rRNA	COI mtDNA	Histone H3	Collections
Limopsis cristata	Jeffreys, 1876					MZSP104154, MCZ348410
Limopsis cumingi	Adams, 1863	KT757802		AB076930		
Limopsis enderbyensis	Powell, 1958	AJ422057	AY321301			
Limopsis galatheae	Knudsen, 1970					MCZ348437
Limopsis lilliei	E A Smith, 1915					MZSP90647, USNM904585
Limopsis marionensis	E A Smith, 1885	AJ422058	AY321303			USNM760835, USNM886526
Limopsis sp.	Sassi, 1827	KC429329	KC429422		KC429164	
Limopsis sulcata	Verrill & Bush, 1898					USNM832925
Limopsis tenella	Jeffreys, 1876					USNM807040
Philobryidae						
Adacnarca nitens	Pelseneer, 1903	KP340836	KT757815		KT757862	MZSP90616, USNM886551
Lissarca notorcardensis	Melvill & Standen, 1907		EF192520	KF612434		MZSP87826, USNM899485
Neocardia sp.	G B Sowerby III, 1892	KT757804	KT757850	KX713486	KT757891	USNM881121, MCZ378927
Philobrya magellanica	(Stempell, 1899)	KP340845	KT757853		KT757895	
Philobrya sublaevis	Pelseneer, 1903	KP340835	KP340812			MZSP90645, USNM882353
Outgroup–Pteriomorphia						

Taxa	**Reference**	**18S rRNA**	**28S rRNA**	**COI mtDNA**	**Histone H3**	**Collections**
Lima lima	(Linnaeus, 1758)	KC429339	KC429434	KC429101	KC429174	USNM 754383
Malleus albus	Lamarck, 1819	KC429334	HQ329464	KC429097	KC429169	MZSP55595
Mytilus edulis	Linnaeus, 1758	KC429331	KC429424	KF644190	KC429166	MZSP120321
Ostrea edulis	Linnaeus, 1758	L49052	AF137047	AF120651	AY070151	USNM836256
Pecten maximus	(Linnaeus, 1758)	L49053	HM630545	KC429102	EU379508	
Pinctada margaritifera	(Linnaeus, 1758)	AB214451	AB214466	AB259166	HQ329296	USNM836493
Pinna carnea	Gmelin, 1791	HQ329375	KJ366067	KJ366325	KC429172	MZSP29040
Outgroup–Bivalvia						
Chione elevata	(Say, 1822)	KC429387	KC429495	KC429136	KC429219	
Macoma balthica	(Linnaeus, 1758)	KC429393	KC429501	KC429141	KC429224	
Margaritifera margaritifera	(Linnaeus, 1758)	AF229612	KC429443	AF303316	KC429185	
Neotrigonia lamarckii	(Gray, 1838)	KC429345	KC429443	KC429105	KC429182	
Nucula sulcuta	Bronn, 1831	AF207642	KC984815	KC984746	KC984777	

Table 2. Evolutionary correlation tests between mantle margin traits and lifestyles in Arcida. The test compares the four-parameter model (independent evolution; h_0) and the eight-parameter models (correlated evolution; h_1, h_2, h_3) between two binary traits, returning the differences in log-likelihood (–logL) with *p* values calculated by 10,000 simulations. Significant differences, *i.e.*, *p* value < α=0.05, indicate a better fit to the model of correlated evolution. Characters and respective states: *first outer fold pigmentation*, absent (0) or present (1); *compound eyes*, absent (0) or present (1); *pigmented eyespots*, absent (0) or present (1); *inner mantle fold development*, up to twice the length (0) or much longer (1) than the first outer fold; *mode of life*, epifaunal (0) or semi-infaunal/infaunal (1).

Morphological traits (y) and hypotheses (h)	**Mode of life – epifaunal vs. infaunal (x)**		
	Difference in –logL *between models*	p *value*	*Conclusion*
First outer fold pigmentation			
h_1 correlation	2.8321	0.138	independent traits
Compound eyes			
h_1 correlation	0.9473	0.268	independent traits
Pigmented eyespots			
h_1 correlation	5.12	0.0223	correlated traits
h_2 x depends on y	0.4789	0.3884	x does not depend on y
h_3 y depends on x	2.0402	0.13	y does not depend on x
Inner mantle fold development			
h_1 correlation	6.4797	0.002	correlated traits
h_2 x depends on y	2.3043	0.0112	x depends on y
h_3 y depends on x	3.1362	0.0569	y does not depend on x

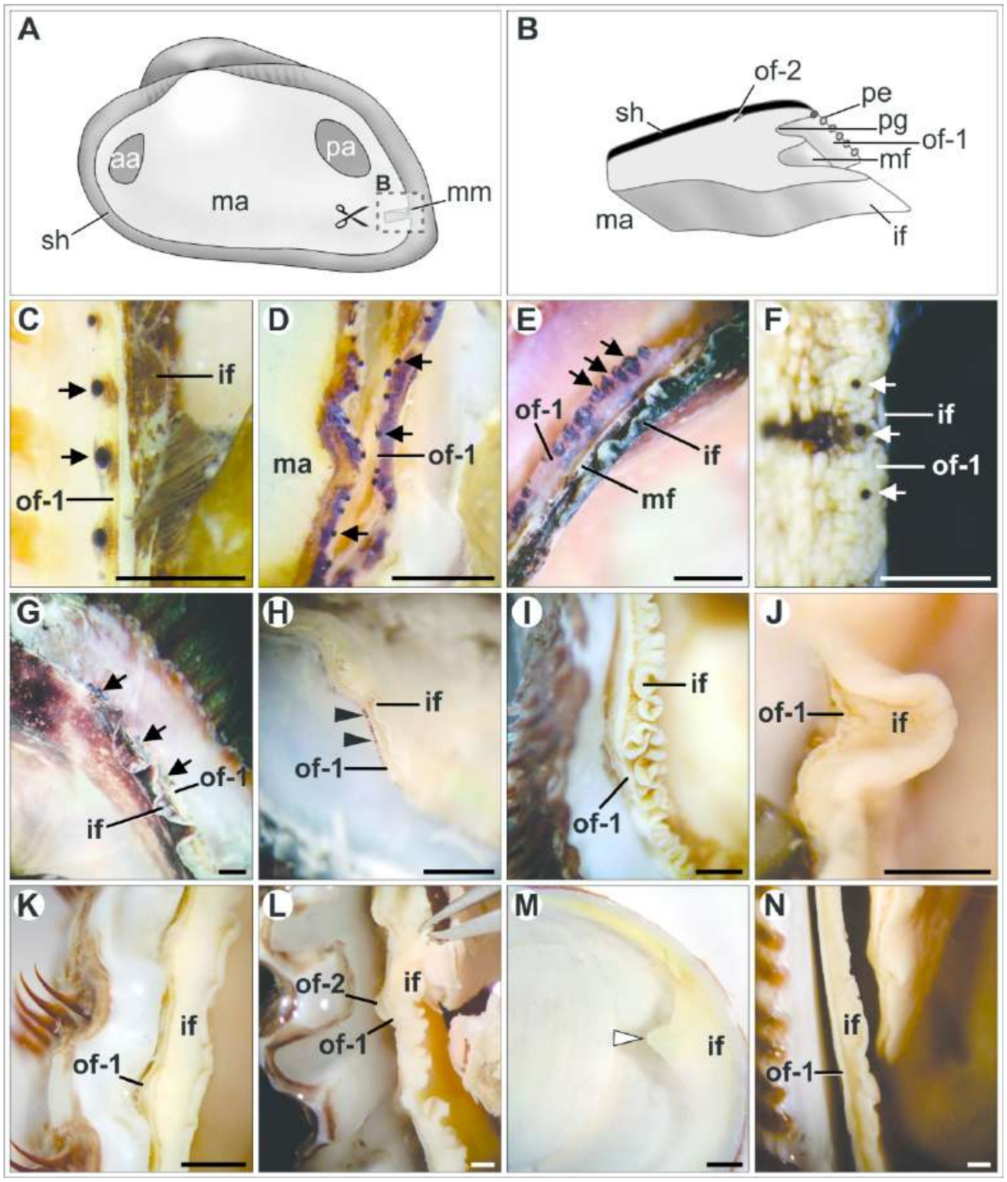

Figure 1. General organization of the mantle (A) and mantle margin (B) in Arcida represented by simplified schemes. Mantle margin morphology in Arcidae (C-E, G-N) and Cucullaeidae (F). Posterior mantle region, ventral view. Scale bars = 1mm. The first outer fold can be pigmented (C-G), bearing multiple compound eyes (arrows) and pigmented eyespots (arrowheads). The middle fold is reduced (E) or absent (J). The inner fold is much longer than the other folds, forming a large curtain (I-N) or a posterior flap (M). C. *Acar plicata* (USNM 886349). D. *Arca noae* (USNM 1086014). E. *Barbatia fusca* (SBMNH 349329). F. *Cucullaea labiata* (USNM 746883). G. *Barbatia barbata* (MCZ 378867). H. *Barbatia virescens* (MCZ 378874). I. *Barbatia candida* (MZSP 105572). J. *Anadara broughtonii* (USNM 802331). K. *Anadara ferruginea* (SBMNH 81002). L. *Tegillarca granosa* (MCZ 378820). M. *Bathyarca corpulenta* (SBMNH 349320). N. *Trisidos kiyonoi* (SBMNH 97422). Abbreviations: aa, anterior adductor; if, inner fold; ma, mantle; mf, middle fold; mm, mantle margin; of, outer fold; of-1, first outer fold; of-2, second outer fold; pa, posterior adductor; pe, pigmented eyespots; pg, periostracal groove; sh, shell.

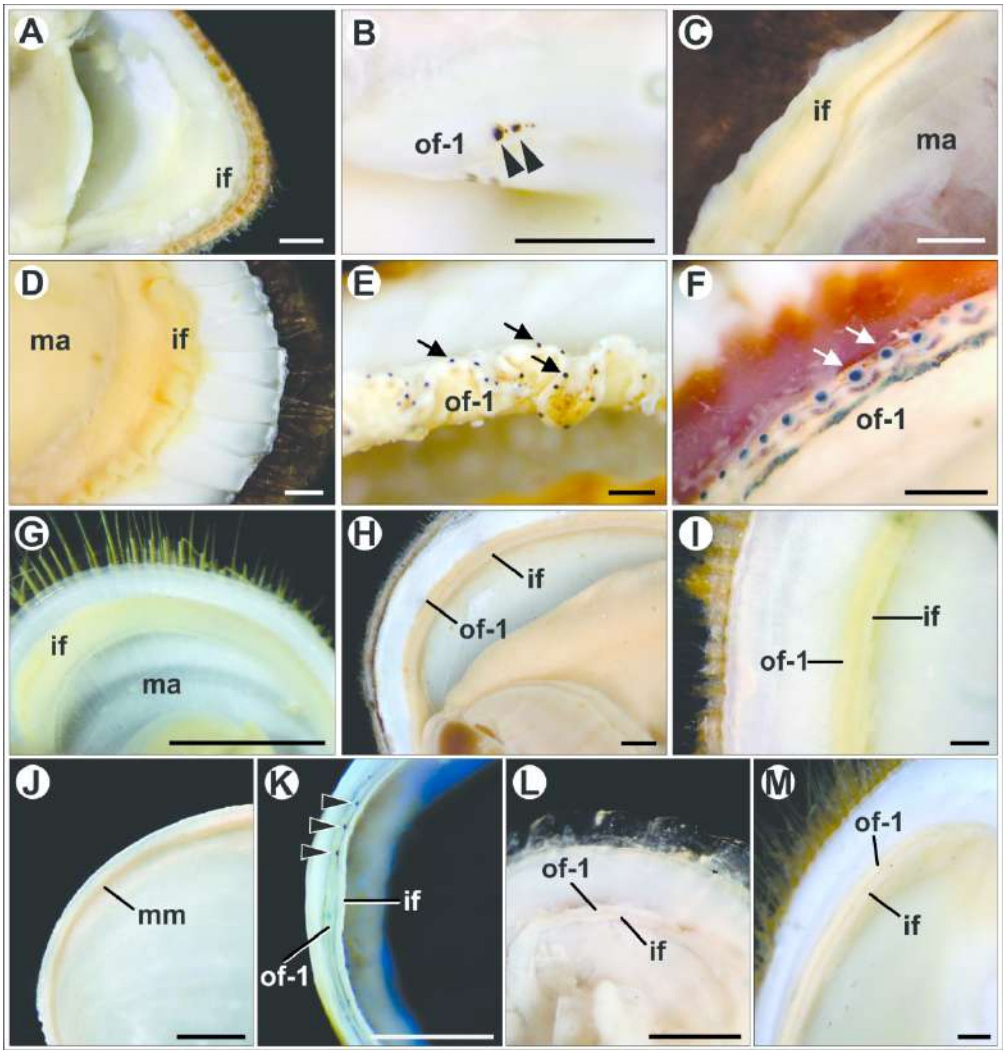

Figure 2. Mantle margin morphology in Noetiidae (A-D), Glycymerididae (E, F), Limopsidae (G-I), and Philobryidae (J-M). Posterior mantle region. Scale bars = 1mm. The first outer fold can bear compound eyes (arrows) and pigmented eyespots (arrowheads). A. *Striarca lactea* (USNM 857645). B. *Arcopsis solida* (USNM 733218). C. *Didimacar tenebrica* (SBMNH 80722). D. *Noetia ponderosa* (USNM 803530). E. *Tucetona pectinata* (MZSP 91971). F. *Glycymeris tenuicostata* (378982). G. *Limopsis aurita* (ZUEC-BIV 2248). H. *Limopsis lilliei* (MZSP 90647). I. *Limopsis marionensis* (USNM 760835). J. *Adacnarca nitens* (USNM 886551). K. *Lissarca notorcadensis* (MZSP 87826). L. *Neocardia sp.* (MCZ 378927). M. *Philobrya sublaevis* (MZSP 90645). Abbreviations: if, inner fold; ma, mantle; mm, mantle margin; of-1, first outer fold.

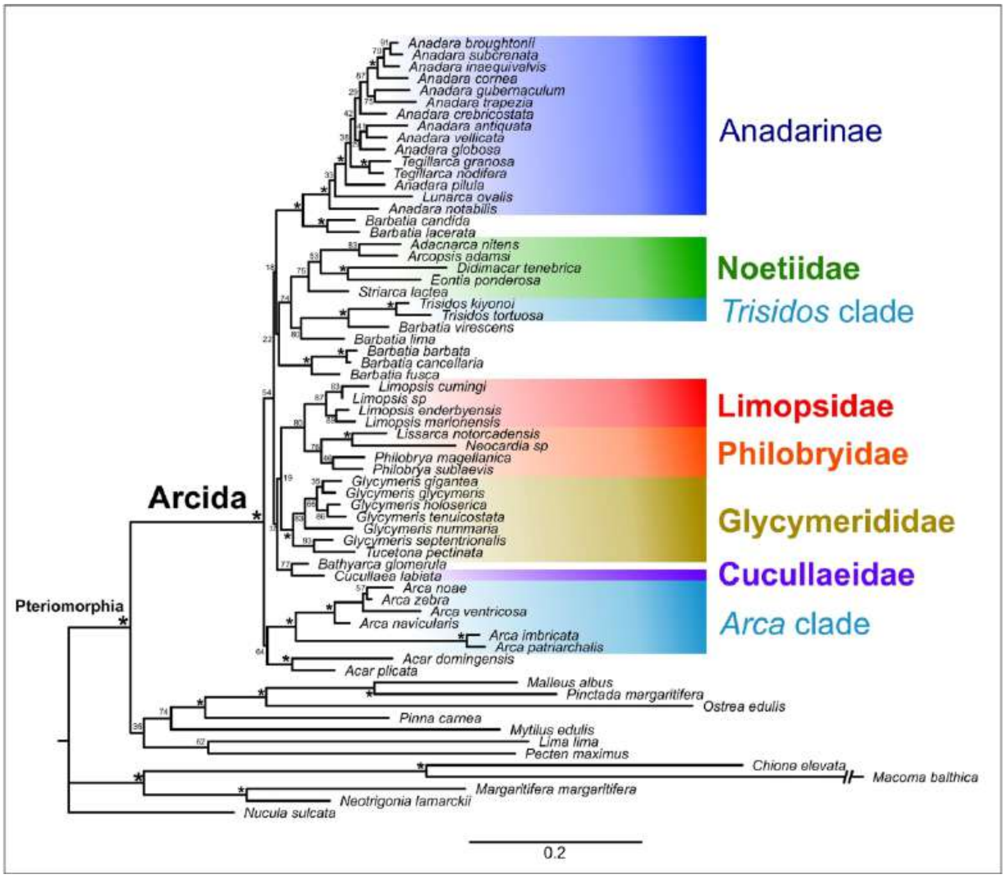

Phylogenetic relationships within Arcida based on maximum likelihood analysis of four genes (18S rRNA, 28S rRNA, COI mtDNA, and H3). Asterisks on nodes indicate bootstrap values > 95%. Selected clades are indicated by color groups. Arcidae is the only non-monophyletic family.

168x146mm (300 x 300 DPI)

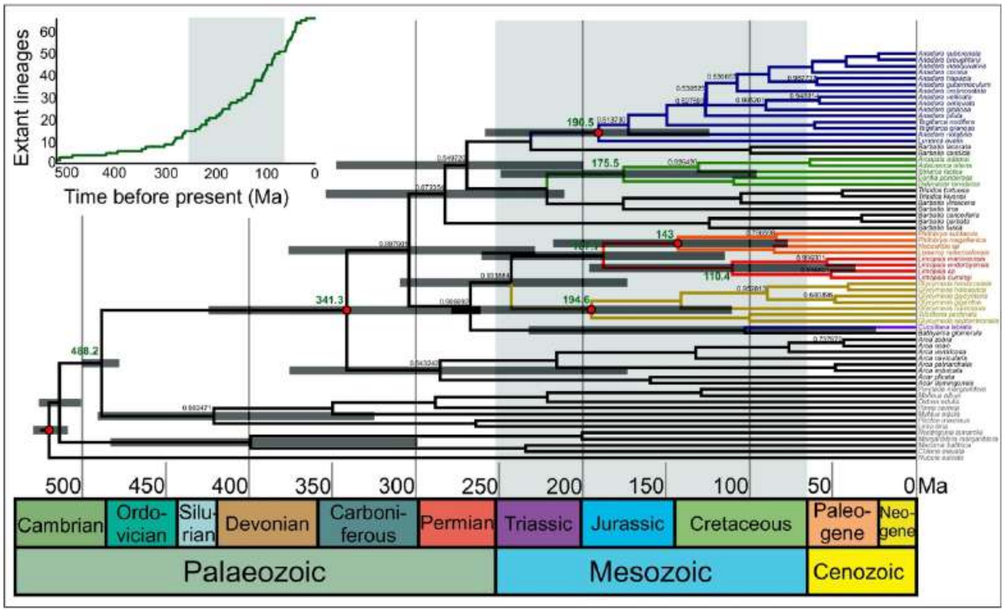

Time-calibrated phylogeny of Arcida under Bayesian inference based on four genes (18S rRNA, 28S rRNA, COI mtDNA, and H3) and five fossils used to calibrate internal nodes (red circles). Green values indicate median ages on selected nodes. Grey bars indicate 95% highest posterior density intervals (HPD) for nodes of interest. Posterior probabilities different than 1.0 are indicated on nodes. Color code for clades and taxa is the same used in Figure 3. A lineages-through-time plot is shown at the upper left (generated in IcyTree – https://icytree.org/). After a Cambrian divergence, the crown group of Arcida had an origin around 341 Ma (Carboniferous) and a major diversification during the Mesozoic.

168x101mm (300 x 300 DPI)

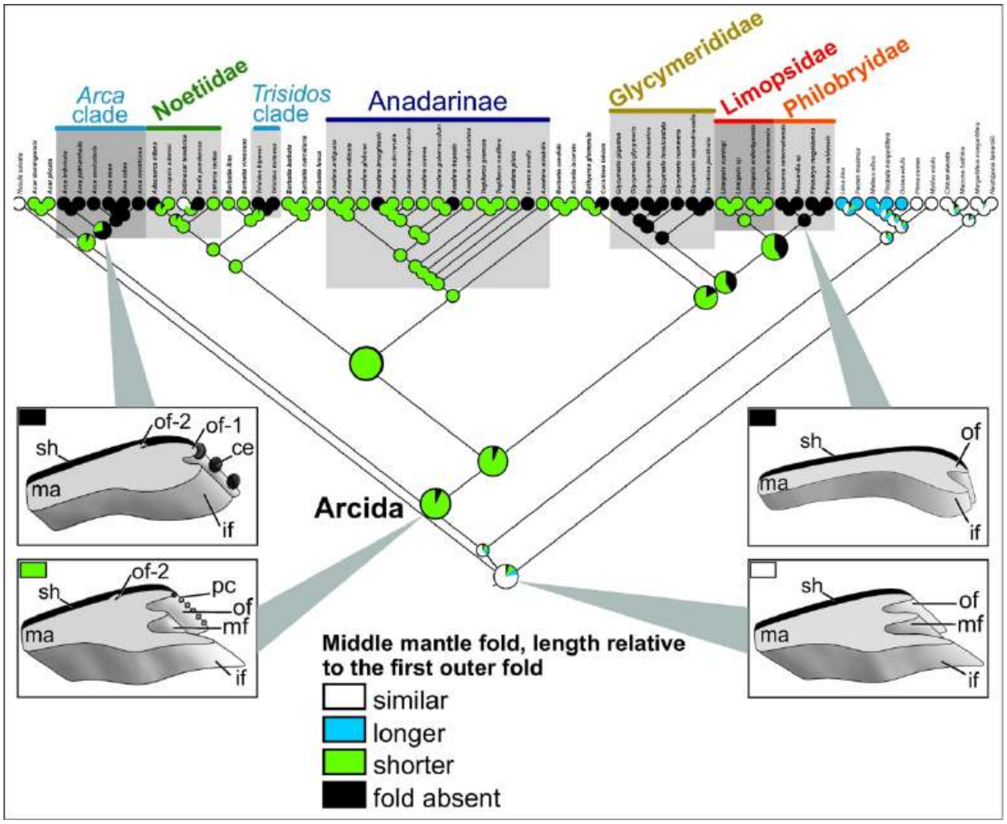

Ancestral state reconstruction of the middle mantle fold in Arcida under maximum likelihood, assuming a single rate for all possible transitions (Mk1 model). Pie charts represent the likelihood proportions of reconstructed states; nodes of interest have their charts enlarged. Mantle margin schemes indicate mantle morphology as reconstructed by the analysis. Abbreviations: ce, compound eyes; if, inner fold; ma, mantle; mf, middle fold; of, outer fold; of-1, first outer fold; of-2, second outer fold; pc, pigmented cups; sh, shell.

168x137mm (300 x 300 DPI)

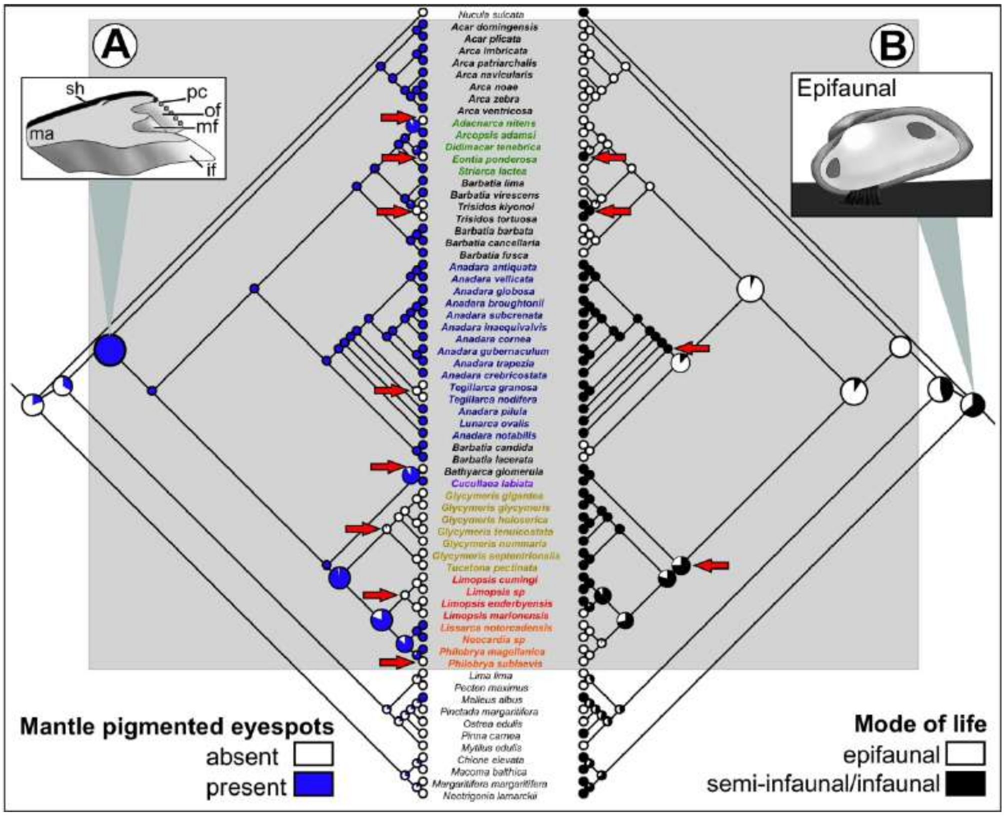

Ancestral state reconstruction of mantle photoreceptor organs (left, AsymmMK model) and mode of life (right, MK1 model) in Arcida under maximum likelihood. Ingroup is indicated by the grey boxes. Pie charts represent the likelihood proportions of reconstructed states; nodes of interest have their charts enlarged. The Arcida's ancestor is recovered as an epifaunal animal with simple eyespots on the mantle. Most subsequent losses of eyespots (red left arrows) are apparently associated with transitions to semi-infaunal/infaunal habits (red right arrows). Abbreviations: if, inner fold; ma, mantle; mf, middle fold; of, outer fold; of-1, first outer fold; pc, pigmented eyespots; sh, shell.

168x136mm (300 x 300 DPI)

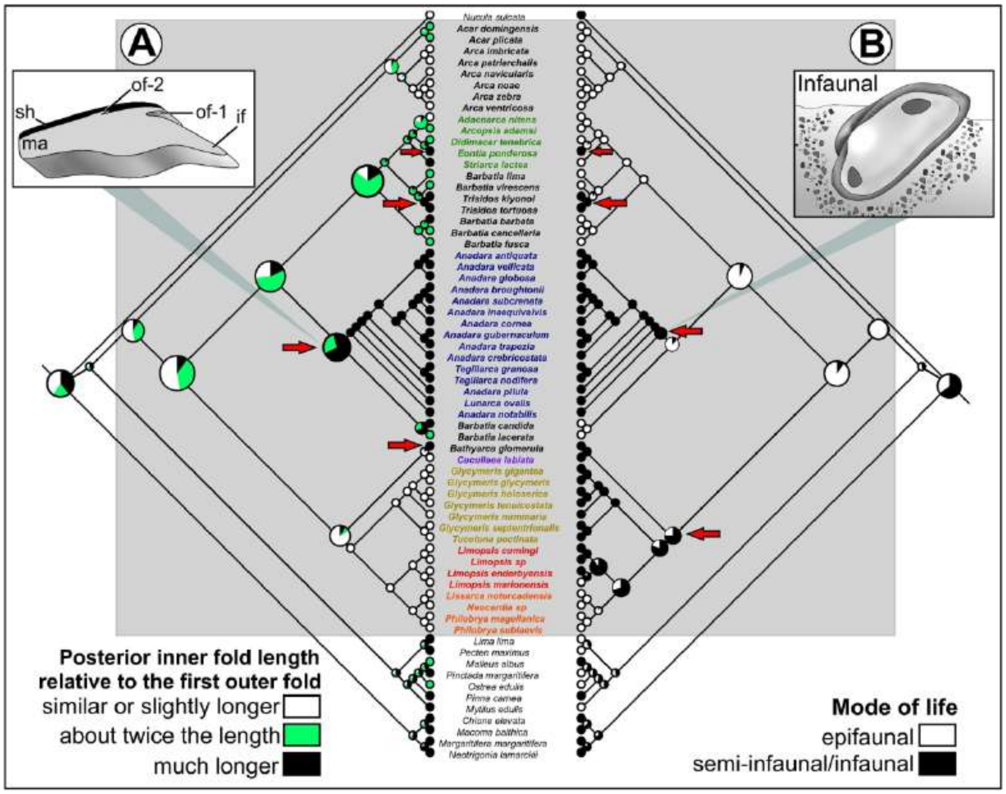

Ancestral state reconstruction of inner fold length (left) and mode of life (right) in Arcida under maximum likelihood, assuming a single rate for all possible transitions (Mk1 model). Pie charts represent the likelihood proportions of reconstructed states; nodes of interest have their charts enlarged. The inner mantle fold becomes much longer than the others in numerous lineages (left arrows), which is apparently associated with transitions to semi-infaunal/infaunal habits (right arrows). Abbreviations: if, inner fold; ma, mantle; of-1, first outer fold; of-2, second outer fold; sh, shell.

168x132mm (300 x 300 DPI)

Supplemental material

Table 1. Characters and states used to study mantle margin traits and lifestyles in Arcida. Abbreviations: IF, inner mantle fold; MF, middle mantle fold; OF, outer mantle fold.

Characters	State 0	State 1	State 2	State 3	State 4
1. Mantle margin, number of folds	3 (1OF, 1MF, 1IF)	3(2OF, 1IF)	4 (2OF, 1MF, 1IF)	2 (1OF, 1IF)	4 (1OF, 1MF, 2IF)
2. Mantle margin, middle mantle fold	present	absent			
3. Mantle margin, circumpallial nerve	absent	present			
4. Mantle margin, pigmentation	absent	uniform	intense posteriorly		
5. Mantle margin, proximal second outer mantle fold	absent	present			
6. Mantle margin, pallial photoreceptor organs	absent	present			
7. Mantle margin, antero-posterior differentiation in relative length and thickness	absent	present			
8. First outer mantle fold, compound eyes	absent	present			
9. First outer mantle fold, pigmented eyespots	absent	present			
10. First outer mantle fold, pigmented pit eyespots	absent	present			
11. First outer mantle fold, pigmented cup eyespots	absent	present			
12. First outer mantle fold, pigmentation	absent	present			
13. Middle mantle fold, length relative to the first outer fold	similar	longer	shorter	fold absent	
14. Middle mantle fold, length relative to the first outer fold (binary)	similar or longer	shorter or absent			
15. Inner mantle fold, posterior length relative to the first outer fold	similar or slightly longer	about twice the length	much longer		
16. Inner mantle fold, posterior length relative to the first outer fold (binary)	up to twice the length	much longer			
17. Mode of life, occurrence relative to depth	shallow waters (<200m)	shallow and deep waters	deep waters (>200m)		
18. Mode of life, position relative to substrate	epifaunal	semi-infaunal	infaunal		
19. Mode of life, position relative to substrate	epifaunal	semi-			

(binary)		infaunal/infaunal	
20. Mode of life, type of substrate (binary)	hard substrate	soft substrate	
21. Mode of life, type of substrate	sandy and muddy	rocks and corals	living organisms
22. Mode of life, use of byssus at adult stage	abyssate	endobyssate	epibyssate

Supplemental material

Table 2. Species-character matrix.

Taxa	**1**	**2**	**3**	**4**	**5**	**6**	**7**	**8**	**9**	**10**	**11**	**12**	**13**	**14**	**15**	**16**	**17**	**18**	**19**	**20**	**21**	**22**
Acar domingensis	2	0	0	1	1	1	1	1	1	1	0	1	2	1	1	0	0	0	0	0	1	2
Acar plicata	2	0	0	1	1	1	1	1	1	1	0	1	2	1	1	0	0	0	0	0	1	2
Adacnarca nitens	3	1	0	0	0	0	0	0	0	0	0	0	3	1	0	0	1	0	0	0	2	2
Anadara antiquata	2	0	0	2	1	1	1	0	1	1	0	1	2	1	2	1	0	2	1	1	0	1
Anadara broughtonii	1	1	0	0	1	1	1	0	1	1	0	0	3	1	2	1	0	2	1	1	0	1
Anadara cornea	2	0	0	0	1	1	1	0	1	1	0	0	2	1	2	1	0	2	1	1	0	1
Anadara crebricostata	2	0	0	0	1	1	1	0	1	1	0	0	2	1	2	1	0	2	1	1	0	1
Anadara globosa	2	0	0	0	1	1	1	0	1	1	0	0	2	1	2	1	0	2	1	1	0	1
Anadara gubernaculum	2	0	0	0	1	1	1	0	1	1	0	0	2	1	2	1	0	2	1	1	0	1
Anadara inaequivalvis	2	0	0	0	1	1	1	0	1	1	0	0	2	1	2	1	0	2	1	1	0	1
Anadara notabilis	2	0	0	0	1	1	1	0	1	1	0	0	2	1	2	1	0	2	1	1	0	1
Anadara pilula	2	0	0	0	1	1	1	0	1	1	0	0	2	1	2	1	0	2	1	1	0	1
Anadara subcrenata	2	0	0	0	1	1	1	0	1	1	0	0	2	1	2	1	0	2	1	1	0	1
Anadara trapezia	1	1	0	0	1	1	1	0	1	1	0	0	3	1	2	1	0	2	1	1	0	1
Anadara vellicata	2	0	0	0	1	1	1	0	1	1	0	0	2	1	2	1	0	2	1	1	0	1
Arca imbricata	1	1	0	2	1	1	1	1	1	1	0	1	3	1	0	0	0	0	0	0	1	2
Arca navicularis	1	1	0	2	1	1	1	1	1	1	0	1	3	1	0	0	0	0	0	0	1	2
Arca noae	1	1	0	2	1	1	1	1	1	1	0	1	3	1	0	0	0	0	0	0	1	2
Arca patriarchalis	1	1	0	2	1	1	1	1	1	1	0	1	3	1	0	0	0	0	0	0	1	2
Arca ventricosa	1	1	0	2	1	1	1	1	1	1	0	1	3	1	0	0	0	0	0	0	1	2
Arca zebra	1	1	0	2	1	1	1	1	1	1	0	1	3	1	0	0	0	0	0	0	1	2
Arcopsis adamsi	2	0	0	0	1	1	1	0	1	1	0	0	2	1	1	0	0	0	0	0	1	2
Barbatia barbata	2	0	0	2	1	1	1	1	1	1	0	1	2	1	2	1	0	0	0	0	1	2
Barbatia cancellaria	2	0	0	2	1	1	1	1	1	1	0	1	2	1	1	0	0	0	0	0	1	2
Barbatia candida	2	0	0	0	1	1	1	0	1	1	0	0	2	1	2	1	0	0	0	0	1	2
Barbatia fusca	2	0	0	2	1	1	1	1	1	1	0	1	2	1	1	0	0	0	0	0	1	2
Barbatia lacerata	2	0	0	0	1	1	1	0	1	1	0	0	2	1	1	0	0	0	0	0	1	2
Barbatia lima	2	0	0	0	1	1	1	0	1	1	0	0	2	1	1	0	0	0	0	0	1	2
Barbatia virescens	2	0	0	0	1	1	1	0	1	1	0	0	2	1	1	0	0	0	0	0	1	2

Taxa	**1**	**2**	**3**	**4**	**5**	**6**	**7**	**8**	**9**	**10**	**11**	**12**	**13**	**14**	**15**	**16**	**17**	**18**	**19**	**20**	**21**	**22**
Bathyarca glomerula	2	0	0	0	1	0	1	0	0	0	0	0	2	1	2	1	1	1	1	1	0	1
Chione elevata	4	0	0	0	0	0	1	0	0	0	0	0	0	0	2	1	0	2	1	1	0	0
Cucullaea labiata	1	1	0	0	1	1	1	1	1	1	0	0	3	1	0	0	0	1	1	1	0	1
Didimacar tenebrica	2	0	0	0	1	1	1	0	1	1	0	0	0	0	1	0	0	0	0	0	1	2
Eontia ponderosa	1	1	0	0	1	0	1	0	0	0	0	0	3	1	2	1	0	2	1	1	0	1
Glycymeris gigantea	1	1	0	2	1	1	1	1	0	0	0	1	3	1	0	0	0	1	1	1	0	0
Glycymeris glycymeris	1	1	0	2	1	1	1	1	0	0	0	1	3	1	0	0	0	1	1	1	0	0
Glycymeris holoserica	1	1	0	2	1	1	1	1	0	0	0	1	3	1	0	0	0	1	1	1	0	0
Glycymeris nummaria	1	1	0	2	1	1	1	1	0	0	0	1	3	1	0	0	0	1	1	1	0	0
Glycymeris septentrionalis	1	1	0	2	1	1	1	1	0	0	0	1	3	1	0	0	0	1	1	1	0	0
Glycymeris tenuicostata	1	1	0	2	1	1	1	1	0	0	0	1	3	1	0	0	0	1	1	1	0	0
Lima lima	0	0	1	1	0	1	0	0	0	0	0	0	1	0	2	1	0	0	0	0	1	2
Limopsis cumingi	0	0	0	0	0	0	0	0	0	0	0	0	2	1	0	0	1	1	1	1	0	1
Limopsis enderbyensis	0	0	0	0	0	0	0	0	0	0	0	0	2	1	0	0	1	1	1	1	0	1
Limopsis marionensis	0	0	0	0	0	0	0	0	0	0	0	0	2	1	0	0	1	0	0	0	1	2
Limopsis sp	0	0	0	0	0	0	0	0	0	0	0	0	2	1	0	0	1	1	1	1	0	1
Lissarca notorcadensis	3	1	0	0	0	1	0	0	1	0	1	0	3	1	0	0	0	0	0	0	2	2
Lunarca ovalis	1	1	0	2	1	1	1	0	1	1	0	1	3	1	2	1	0	2	1	1	0	1
Macoma balthica	0	0	0	0	0	0	1	0	0	0	0	0	0	0	2	1	0	2	1	1	0	0
Malleus albus	2	0	1	1	0	1	0	0	1	0	1	0	1	0	1	0	0	1	1	1	0	1
Margaritifera margaritifera	0	0	0	2	0	0	1	0	0	0	0	0	0	0	2	1	0	1	1	1	0	0
Mytilus edulis	0	0	1	2	0	0	1	0	0	0	0	0	0	0	2	1	0	0	0	0	1	2
Neocardia sp	3	1	0	0	0	1	0	0	1	0	1	0	3	1	0	0	0	0	0	0	2	2
Neotrigonia lamarckii	0	0	0	0	0	0	1	0	0	0	0	0	0	0	2	1	0	2	1	1	0	0
Nucula sulcata	0	0	0	0	0	0	0	0	0	0	0	0	0	0	0	0	1	2	1	1	0	0
Ostrea edulis	0	0	1	1	0	0	0	0	0	0	0	0	1	0	1	0	0	0	0	0	1	2
Pecten maximus	0	0	1	1	0	1	0	0	0	0	0	0	1	0	2	1	0	0	0	1	0	2
Philobrya magellanica	1	1	0	0	1	1	0	0	1	0	1	0	3	1	0	0	0	0	0	0	2	2
Philobrya sublaevis	1	1	0	0	1	0	0	0	0	0	0	0	3	1	0	0	0	0	0	0	2	2
Pinctada margaritifera	0	0	1	1	0	0	0	0	0	0	0	0	1	0	2	1	0	0	0	0	1	2
Pinna carnea	0	0	1	2	0	0	1	0	0	0	0	0	0	0	2	1	0	1	1	1	0	1
Striarca lactea	2	0	0	0	1	1	1	0	1	1	0	0	2	1	2	1	0	0	0	0	1	2
Tegillarca granosa	2	0	0	0	1	0	1	0	0	0	0	0	2	1	2	1	0	2	1	1	0	1

Taxa	**1**	**2**	**3**	**4**	**5**	**6**	**7**	**8**	**9**	**10**	**11**	**12**	**13**	**14**	**15**	**16**	**17**	**18**	**19**	**20**	**21**	**22**
Tegillarca nodifera	2	0	0	0	1	0	1	0	0	0	0	0	2	1	2	1	0	2	1	1	0	1
Trisidos kiyonoi	1	1	0	0	1	0	1	0	0	0	0	0	3	1	2	1	0	1	1	1	0	1
Trisidos tortuosa	1	1	0	0	1	0	1	0	0	0	0	0	3	1	2	1	0	1	1	1	0	1
Tucetona pectinata	1	1	0	2	1	1	1	1	0	0	0	1	3	1	0	0	0	1	1	1	0	0

Supplemental material

Table S3. Lifestyle compilation of ark clams and relatives (Arcida) according to mode of life (position relative to the substrate & mode of attachment) and substrate.

Taxa	**Mode of life**		**Substrate**	**References**
Arcidae				
Acar domingensisi	Epifaunal	Epibyssate	Rocks	Simone and Chichverkrun 2004
Acar plicata	Epifaunal	Epibyssate	Mud, rubble, shell-hash, under corals	Kilburn 1983, Leung and Morton 2000
Anadara antiquata	Semi-infaunal	Endobyssate	Muddy sand, rock or coral fragments	Evseev and Lutaenko 1998, Broom 1985, Kilburn 1983
Anadara broughtonii	Infaunal	Endobyssate	Mud	Broom 1985, Oliver and Holmes 2006
Anadara cebricostata	Infaunal	Endobyssate		Oliver and Holmes 2006
Anadara cornea	Infaunal	Endobyssate	Mud and sand	Broom 1985, Tsi and Ma 1982, Li and Gao 1985, Morton 1986
Anadara globosa	Infaunal	Endobyssate		Oliver and Holmes 2006
Anadara gubernaculum	Infaunal	Endobyssate	Sand and silty sand	Evsee and Lutaenko 1998, Oliver and Holmes 2006
Anadara ferruginea	Infaunal	Endobyssate	Coarse sand, fine sand, and silty clay	Tsi and Ma 1982, Ong Che and Morton 1991, Scott 1994, Morton 1994, Leung and Morton 1997, 200, Nicholson and Morton 2000
Anadara inequivalvis	Infaunal	Endobyssate	Sand and muddy sand	Broom 1985, Tsi and Ma 1982, Scott 1994, Nicholson and Morton 2000

Taxa	**Mode of life**		**Substrate**	**References**
Anadara notabilis	Infaunal	Endobyssate	Sand	Rocha and Martins 1998, Oliver and Holmes 2006, Tugeon et al. 2009
Anadara ovalis	Infaunal	Endobyssate	Sand	Oliver and Holmes 2006, Alexander 2007, Turgeon et al. 2009
Anadara pilula	Infaunal	Endobyssate	Sand and silty sand	Evsee and Lutaenko 1998, Norte-Campos et al. 2005, Oliver and Holmes 2006
Anadara subcrenata	Infaunal	Endobyssate	Mud and muddy sand	Broom 1985, Oliver and Holmes 2006
Anadara trapezia	Infaunal	Endobyssate	Sandy mudflats	Sullivan 1960, Oliver and Holmes 2006
Anadara vellicata	Infaunal	Endobyssate	Silty sand	Evsee and Lutaenko 1998, Oliver and Holmes 2006
Arca imbricata	Epifaunal	Epibyssate	Rock crevices	Oliver and Holmes 2006, Pers. Obs., Turgeon et al. 2009
Arca navicularis	Epifaunal	Epibyssate	Rocks and coral fragments	Kilburn 1983
Arca noae	Epifaunal	Epibyssate	Rocks	Thomas 1996, Oliver and Holmes 2006, Morton and Peharda 2008
Arca patriarchalis	Epifaunal	Epibyssate	Coral fragments	Dudgeon and Morton 1982
Arca ventricosa	Epifaunal	Epibyssate	Coral fragments	Kilburn 1983, Oliver and Holmes 2006
Arca zebra	Epifaunal	Epibyssate	Rocks	Olvier and Holmes 2006, Turgeon et al. 2009
Barbatia barbata	Epifaunal	Epibyssate	Rocks	Thomas 1996, Oliver and Holmes 2006, Turgeon et al. 2009
Barbatia cancellaria	Epifaunal	Epibyssate	Rocks	Simone and Chichverkrun 2004

Taxa	**Mode of life**		**Substrate**	**References**
Barbatia candida	Epifaunal	Epibyssate	Rocks	Simone and Chichverkrun 2004, Turgeon et al. 2009, Pers.Obs.
Barbatia fusca	Epifaunal	Epibyssate	Coral fragments	Sanpanich 2011, Tsi and Ma 1982. Barbatia decussata. Oliver and Holmes 2006.
Barbatia lacerata	Epifaunal	Epibyssate	Corals, rubble, and rocks	Oliver et al. 2004
Barbatia lima	Epifaunal	Epibyssate	Rocks	Scott 1994, Leung and Morton 2000
Barbatia setigera	Epifaunal	Epibyssate	Coarse sand	Kilburn 1983
Barbatia virescens	Epifaunal	Epibyssate	Rocks, piers and boulders	Morton 1987, Britton 1990, Taylor and Morton 1996, Harper and Morton 1997
Bathyarca glomerula	Semi-infaunal	Endobyssate	Soft sediments	Oliver and Allen 1980, Turgeon et al. 2009
Cucullaea labiata	Semi-infaunal	Endobyssate	Sand and corals	Morton 1981, Oliver and Holmes 2006, Sanpanich 2011
Tegillarca granosa	Infaunal	Endobyssate	Muddy sand	Evsee and Lutaenko 1998, Broom 1985, Morton 1986
Tegillarca nodifera	Infaunal	Endobyssate	Mud, sand, and soft clay	Evsee and Lutaenko 1998
Trisidos kiyonoi	Semi-infaunal	Endobyssate	Gravelly sand and coarse sand	Scott 1994
Noetiidae				
Arcopsis adamsi	Epifaunal	Epibyssate	Rocks on sand	Oliver and Järnegren 2004, Pers. Obs.
Didimacar tenebrica	Epifaunal	Epibyssate	Rocks and boulders	Oliver 1990, Scott 1994, Harper and Morton 1997, Leung and Morton 2000

Taxa	**Mode of life**		**Substrate**	**References**
Noetia ponderosa	Infaunal	Endobyssate	Soft sediments	Oliver 1990
Striarca lactea	Epifaunal	Epibyssate	Rocks, boulders, and among gravel	Oliver and Holmes 2006, Turgeon et al. 2009
Glycymerididae				
Glycymeris gigantea	Semi-infaunal	Free living/ burrower	Coarse shell gravel, sand, and mud	Thomas 1995, 1996, Oliver and Holmes 2006
Glycymeris glycymeris	Semi-infaunal	Free living/ burrower	Coarse shell gravel, sand, and mud	Thomas 1995, 1996, Oliver and Holmes 2006
Glycymeris holoserica	Semi-infaunal	Free living/ burrower	Coarse shell gravel, sand, and mud	Thomas 1995, 1996, Oliver and Holmes 2006
Glycymeris nummaria	Semi-infaunal	Free living/ burrower	Coarse shell gravel, sand, and mud	Thomas 1995, 1996, Oliver and Holmes 2006
Glycymeris septentrionalis	Semi-infaunal	Free living/ burrower	Coarse shell gravel, sand, and mud	Thomas 1995, 1996, Oliver and Holmes 2006
Glycymeris tenuicostata	Semi-infaunal	Free living/ burrower	Coarse shell gravel, sand, and mud	Thomas 1995, 1996, Oliver and Holmes 2006
Tucetona pectinata	Semi-infaunal	Free living/ burrower	Coarse shell gravel, sand, and mud	Turgeon et al. 2009
Limopsidae				
Limospsis sp.	Semi-infaunal	Endobyssate	Soft sediments	Oliver and Allen 1980, Morton 2012, Linse 2014
Limopsis marionensis	Epifaunal	Epibyssate	Associated with sponges and rocks	Cattaneo-Vietti et al. 2000, Narchi et al. 2002, Pörtner et al. 1999
Philobryidae				

Taxa	**Mode of life**		**Substrate**	**References**
Adacnarca nitens	Epifaunal	Epibyssate, epibiotic	Sand, rocks, hydrozoans, bryozoans, sponges, ascidians, and gorgonians	Cattaneo-Vietti et al. 2000, Higgs et al. 2009, Pers. Obs.
Lissarca notorcardensis	Epifaunal	Epibyssate, epibiotic	Spines of cidaroid sea urchins	Brey et al. 1993, Linse et al. 2007
Neocardia sp.	Epifaunal	Epibyssate, epibiotic	Associated with phytals	Lasiak 1999
Philobrya sublaevis	Epifaunal	Epibyssate, epibiotic	Algae	Cattaneo-Vietti et al. 2000

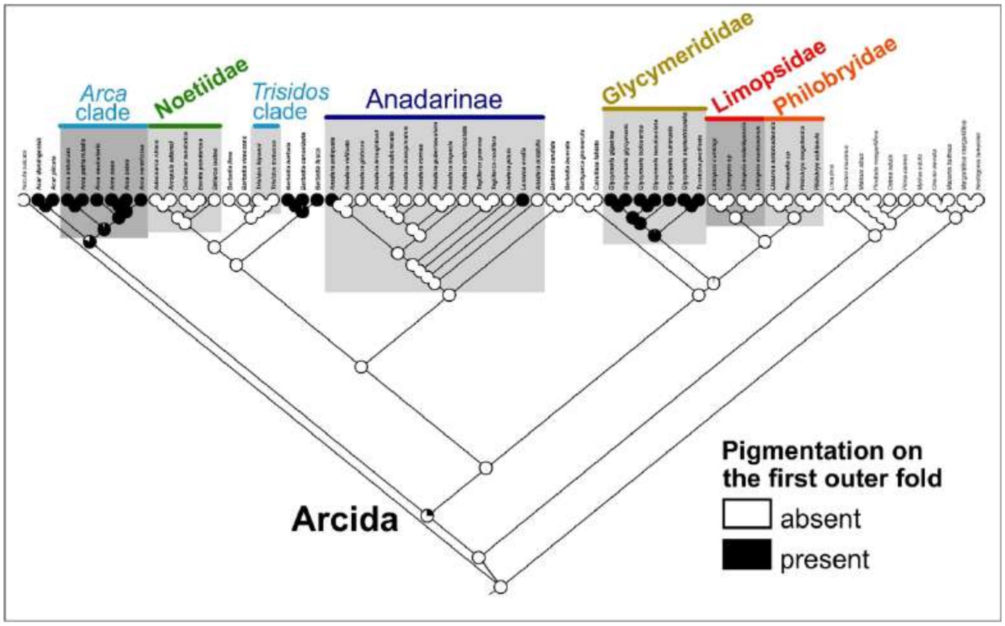

168x104mm (300 x 300 DPI)

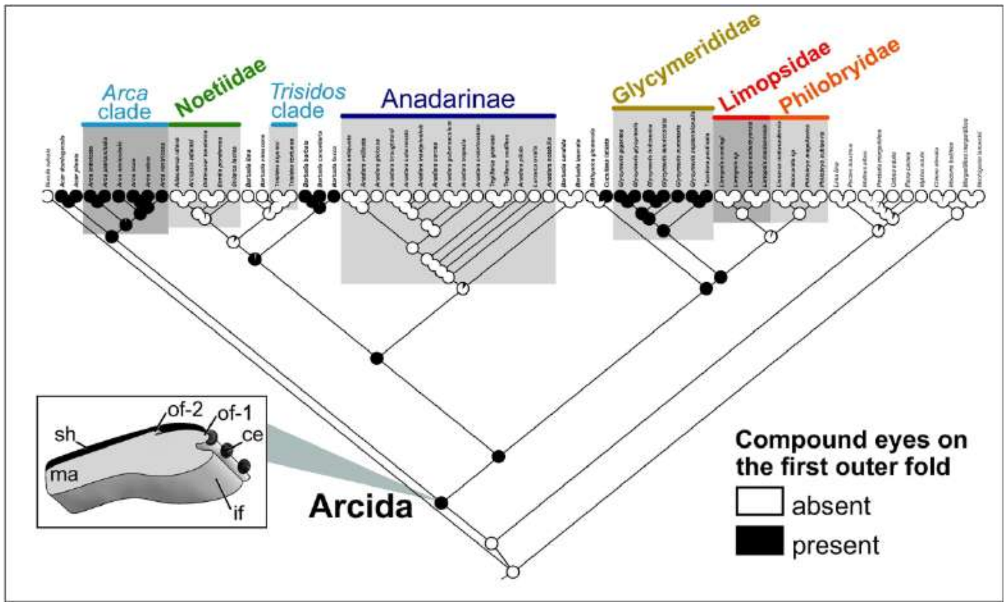

168x100mm (300 x 300 DPI)